applied sciences

MDPI

Review

Implantable Medical Electronic Devices: Sensing Mechanisms, Communication Methods, and the Biodegradable Future

Zhengdao Chu, Yukai Zhou, Saite Li, Qiaosheng Xu and Lijia Pan *

Collaborative Innovation Center of Advanced Microstructures, School of Electronic Science and Engineering, Nanjing University, Nanjing 210023, China; 502023230020@smail.nju.edu.cn (Z.C.)
* Correspondence: ljpan@nju.edu.cn

Abstract

In the context of the relentless pursuit of precision, intelligence, and personalization within the realm of medical technology, the real-time monitoring of human physiological signals has assumed heightened significance. Implantable wireless sensor devices have exhibited extraordinary capabilities in tracking internal physiological parameters, including intraocular pressure, blood glucose levels, electrocardiographic activity, and arterial blood pressure. These devices are characterized by elevated temporal continuity and exceptional measurement accuracy. This paper undertakes an in-depth investigation into the key technologies underlying biodegradable implantable sensing devices. Initially, it expounds on diverse sensing mechanisms employed in implantable devices. Additionally, it presents common data transmission and power supply strategies for wireless sensing systems. Finally, it introduces biodegradable materials suitable for human implantation and their respective application domains and enumerates several implantable devices that are either under development or have already been commercialized. Through an in-depth and comprehensive discourse on the current state of development and extant challenges in this domain, the development trajectory of biodegradable devices is put forward. Moreover, this paper also serves as a valuable reference for the design and selection of implantable medical devices.

Keywords: biomedical sensors; implantable sensors; biodegradable sensors; biocompatibility; wireless transmission

check for updates

Academic Editors: Iman Farhat and Lourdes Farrugia

Received: 20 May 2025
Revised: 30 June 2025
Accepted: 4 July 2025
Published: 7 July 2025

Citation: Chu, Z.; Zhou, Y.; Li, S.; Xu, Q.; Pan, L. Implantable Medical Electronic Devices: Sensing Mechanisms, Communication Methods, and the Biodegradable Future. *Appl. Sci.* **2025**, *15*, 7599. https://doi.org/10.3390/app15137599

Copyright: © 2025 by the authors. Licensee MDPI, Basel, Switzerland. This article is an open access article distributed under the terms and conditions of the Creative Commons Attribution (CC BY) license (https://creativecommons.org/licenses/by/4.0/).

1. Introduction

The advancement of wearable and implantable devices has facilitated the conversion of diverse physiological signals within the human body into unified electrical signals. This transformation is accomplished via the reading of distinct bioelectronic interfaces. Depending on the nature of the signals to be detected, sensors employ different sensing principles. For instance, there exist mechanical signals (such as blood pressure signals, muscle contraction signals, respiratory signals), chemical signals (glucose signals, dopamine signals, lactate signals, oxygen signals), and bioelectrical signals (electrocardiogram signals, electromyogram signals, electroencephalogram signals), among others. These signals are converted into standardized electrical signals through various sensor interfaces and subsequently collected for storage or transmission. Thereafter, they are uploaded to a data center for analysis. This analysis is of paramount importance for discerning human physiological phenomena. Analyzing physiological signals contributes to a deeper understanding of the human body.

Bio-implantable devices exhibit a wide range of application scenarios, encompassing daily monitoring, disease diagnosis, postoperative recovery, and so forth. In recent years, there has been a continuous upsurge in discussions regarding implantable devices, and the enthusiasm for research has remained robust. Researchers have developed implantable sensors with diverse principles and structures. These sensors are capable of continuously monitoring the target signal, featuring a compact size, portability, minimal interference with daily life, extremely low energy consumption, and long-term operation.

However, the development of these devices encounters numerous challenges. Firstly, there are biocompatibility concerns. It is essential to utilize materials with excellent biocompatibility and minimize inflammatory responses. Secondly, issues related to the secure collection and transmission of data exist. Ensuring the accuracy and privacy of data is of utmost importance. Thirdly, power supply problems need to be addressed. This necessitates the development of reliable long-term power supply solutions or self-power supply technologies. Additionally, challenges regarding the long-term stability and reliability of the devices must be considered. Published reviews on implanted devices also delve into these matters. For instance, implanted devices are influenced by motion artifacts. Decisions need to be made regarding the flexibility, durability, and human adaptability of biomaterials, along with the performance requirements of implanted batteries and their potential effects on the human body. Moreover, discussions have also taken place regarding concerns about the privacy and information security of medical data in the era of the Internet of Things.

As the nucleus of the entire system, the sensing unit assumes a pivotal role. To effectively monitor diverse signals, a meticulous selection of the most appropriate sensing mechanism is imperative. For instance, when it comes to monitoring internal pressure signals within the human body, resistive, capacitive, LC resonant, and piezoelectric sensors can be employed, each of which exhibits distinct advantages and limitations. Resistive pressure sensors can be fabricated to a remarkably small size, rendering them highly conducive for implantation in the human body. Nevertheless, their resistance demonstrates relatively high sensitivity to temperature variations, thereby necessitating temperature compensation. Moreover, their sensitivity is generally low [1]. Capacitive sensors feature higher sensitivity and are well-suited for low-pressure monitoring. However, they typically occupy a relatively large area and are susceptible to parasitic capacitance. LC resonant sensors obviate the need for wired connections and are amenable to miniaturization. Nevertheless, wireless signals experience significant attenuation within the human body, and precise external equipment is indispensable for signal reception and processing [2]. Piezoelectric sensors possess the distinct advantage of self-power supply, obviating the need for a battery. They exhibit a relatively rapid response speed, rendering them highly suitable for dynamic monitoring applications. Nevertheless, these sensors are not without limitations. Specifically, the output signal is feeble and necessitates amplification, and piezoelectric materials may elicit rejection reactions when in contact with human tissues. Consequently, it is of paramount importance to select different principles based on the location of the target signal and the characteristics of the device.

To accomplish the all-day measurement of physiological signals, the crux lies in the realization of wireless communication and wireless power supply, along with the real-time transmission of the measured data to the terminal. At present, the commonly employed medical detection devices are typically connected to the equipment via wires or optical cables. This connection approach is straightforward, practical, and cost-effective, and it can effectively mitigate external interference. Nevertheless, it is evident that this method is not applicable to implantable devices, as it will impose significant inconvenience on the subjects. Furthermore, continuous monitoring becomes unfeasible when the subjects engage in certain activities. The utilization of wireless communication can concurrently

address these two issues. For individuals at potential disease risk, including those who require blood glucose, blood pressure [2–4], and intracranial pressure [5,6] monitoring, implantable devices empower them to perform round-the-clock monitoring in their daily lives, obviating the necessity of regular hospital visits for such monitoring. This approach not only mitigates the disruption to patients' daily routines but also facilitates the collection of human physiological data under real-world conditions, which holds great significance for disease surveillance and prevention.

The choice of wireless transmission and wireless power supply techniques is a pivotal determinant in attaining optimal sensing performance without disrupting the wearer's normal daily activities. Given the diverse locations of various implanted devices, the interference they encounter also varies significantly. Consequently, the suitable communication methods also diverge accordingly. Regarding active devices, technologies including Near Field Communication (NFC), Bluetooth, Radio Frequency Identification (RFID), and infrared can be utilized. In the case of passive devices, data transmission can be accomplished via ultrasonic energy transmission or electromagnetic induction coupling (LC resonance) approaches. Each communication method makes use of electrical signals within specific frequency bands, and the absorption and scattering of these signals in human tissues also differ. Devices implanted beneath the skin are subject to relatively less interference. Consequently, they necessitate a shorter communication range and lower power consumption. In contrast, sensors implanted deep within the human body, such as in arteries or vital organs, are confronted with more interference and thus demand higher power to attain a longer communication distance. This calls for designers to meticulously select the communication method and frequency band. Simultaneously, they should also endeavor to prevent electromagnetic radiation and thermal damage to the human body resulting from high-power data transmission. The power supply unit constitutes a crucial component of wireless sensors. Nevertheless, the capacity of batteries remains relatively constrained. In the case of long-term implanted devices, multiple surgical procedures may be necessary to replace the battery, which can inflict harm on the wearer. Regarding biodegradable electronic devices, chemical batteries are non-biodegradable. During the degradation process of the outer casing, the heavy metals contained therein can pose serious chemical risks to the human body. Consequently, the development of a wireless power supply scheme for implanted devices represents an important issue that demands urgent attention. Battery-free systems exhibit a greater ability to conform to human tissues while concurrently reducing the system's volume. The power source of such systems can be derived either from within the body [7–10] or from external sources [11–13]. During the actual design phase, it is essential to take into account the device's practical usage as well as the pros and cons of each scheme.

For implantable sensors engineered for short-term monitoring purposes, such as assessing the postoperative recovery status, devices fabricated and encapsulated with biodegradable materials offer substantial advantages. These devices will spontaneously degrade after functioning appropriately within the body for a specific duration, which can range from several days to a few weeks. The degradation products are either assimilated by the human body or excreted harmlessly from the body. This obviates the necessity for a secondary surgical procedure to remove the device and minimizes the potential harm to the patient's body to the greatest possible extent.

This article conducts a comprehensive review of the most recent advancements in biodegradable wireless implantable sensors and meticulously analyzes the pros and cons of different sensing techniques. Concerning wireless data transmission and wireless power supply, this paper presents several currently prevalent wireless communication implementations approaches and contrasts their applicable scopes. Additionally, this article puts forward strategies for powering sensors without batteries, enabling diverse types of

devices to choose appropriate solutions. Furthermore, this article places particular emphasis on the performance and selection strategies of biodegradable materials. A variety of biodegradable materials and their degradation characteristics are enumerated in the article, offering references and convenience for the design of biodegradable devices. The article deliberates on each of the aforementioned modules and introduces the development status of implantable sensors, implantable miniature antennas, and biodegradable materials.

Research Method

This review centers on research papers pertaining to implantable sensors over the past five years and incorporates publicly accessible data of certain commercially available sensors. Through systematic sorting and integration of relevant materials in recent years, it conducts a profound analysis of the advantages and limitations manifested in the selection of different sensing mechanisms, communication methods, and biodegradable materials during the design and manufacturing processes of implantable sensors. In the realm of sensor design, distinct sensing mechanisms each possess unique applicable ranges and physical quantities amenable to detection; different communication methods correspond to specific requirements regarding implantation distance and communication rate; and the selection of diverse biodegradable materials necessitates a comprehensive consideration of factors such as the implantation environment and the anticipated implantation duration. This paper predominantly employs a research approach integrating qualitative and quantitative analyses to elaborate meticulously on the optimal applicable environments of various modes and presents some crucial data. All data are sourced from references, and in-depth interpretations and comparative analyses of data under different modes are also executed. The objective is to aid readers in designing sensors that meet their specific needs based on the data summarized herein, thereby enabling the functions and structures of sensors to more readily attain the design objectives.

2. Sensing Method

2.1. Magnetic Field Sensing

2.1.1. Applied Technologies

Magnetic field sensors typically achieve sensing based on the Hall effect. The Hall effect is the phenomenon in which, when an electric current passes through a conductor placed in a magnetic field, the charge carriers are influenced by the Lorentz force, leading to the generation of an electromotive force on both sides of the conductor. Implantable Hall sensors accurately utilize this principle to acquire magnetic field information by measuring the Hall electromotive force. Magnetic field sensors exhibit a high degree of sensitivity to variations in the magnetic field and are capable of detecting feeble magnetic fields, thereby demonstrating high sensitivity. Simultaneously, a certain distance exists between the sensor and the object under measurement, enabling non-contact measurement. Nevertheless, this type of device is susceptible to interference from external magnetic fields, which may lead to errors, necessitating calibration. Moreover, magnetic materials are sensitive to temperature fluctuations, and the impact of temperature changes on the measurement results must be taken into account [14].

Based on the Hall effect, Magkoutas developed an extravascular magnetic flux sensing device [15]. This device can continuously monitor arterial blood pressure (ABP), arterial wall diameter (AD), and arterial circumferential strain (ACS). Moreover, it can additionally derive physiological data such as pulse wave velocity, respiratory rate, and the duration of the cardiac systolic phase. This device consists of a Hall effect sensor and a miniature magnet, which are placed on the outer wall of the blood vessel and separated by a certain distance (Figure 1a). As the heart beats, the distance between these two components

changes periodically. By means of the shift in the magnetic field magnitude on the Hall effect sensor, ABP, AD, and ACS can be calculated. Based on the aortic blood pressure waveform, the respiratory rate and the systolic phase of the cardiac cycle can also be deduced. When multiple identical sensors are implanted at different positions in the human body, the pulse wave velocity (PWV) can be measured by means of the time difference in the signals detected by the sensors. This device can be placed in a housing that is 3D printed with biocompatible materials. The housing has been optimized for different blood vessel diameters to ensure precise installation at the designated site and accurate measurement.

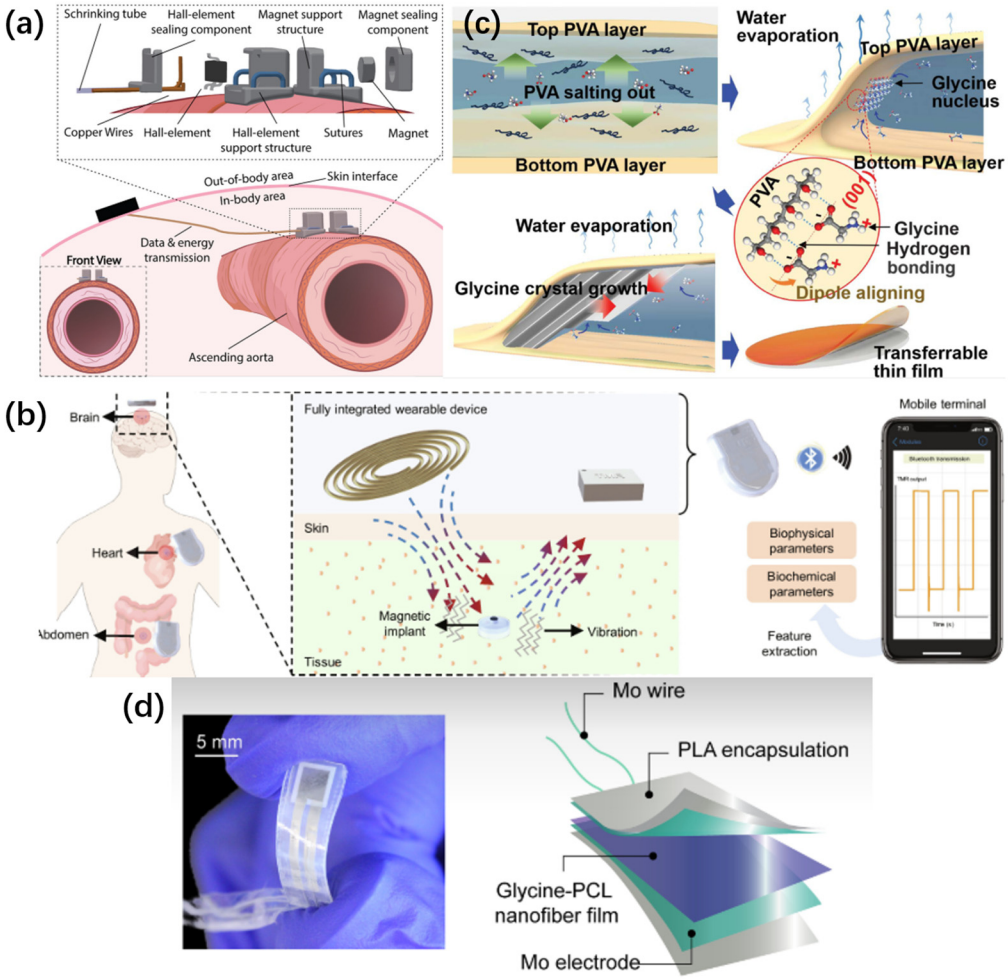


Figure 1. (**a**) Illustration of the hall-based sensing device attachment and a detailed view showing the components comprising the sensing device. The hall-effect sensor and magnet are completely separated, and they are sutured at a predefined distance on the outer arterial wall. (**b**) Millimeter-scale magnetic implants can achieve two-way wireless communication with fully integrated wearable devices, and data collection and processing can be completed on mobile devices. (**c**) The figure shows the crystallization process of the glycine-polyvinyl alcohol interlayer film. During the nucleation stage, glycine molecules exhibit a specific orientation arrangement on the surface of polyvinyl alcohol (PVA), and this arrangement further triggers the ordered arrangement of long-range crystals. (**d**) A glycine-polycaprolactone (PCL) ultrasonic transducer with fully biodegradable properties. The device mainly consists of a piezoelectric glycine-polycaprolactone (PCL) pad, molybdenum electrodes and wires, and a polylactic acid (PLA) encapsulation layer.

Based on the principle that vibration gives rise to a pulsed magnetic field, Wan developed a millimeter-scale, chip-free, and battery-free magnetic implant system [16]. This system wirelessly induces the large-amplitude vibration of the magnetic implant. Sub-

sequently, the damped vibration of the magnetic implant generates a dynamic magnetic field, which can be detected by the magnetic sensors integrated in wearable devices. For magnetic implants with sealed or open cavities, the higher the viscosity of the surrounding environment, the greater the vibration damping and the quicker the vibration attenuation. These motions reflect the biophysical conditions surrounding the implant and the concentration of specific biochemical substances (Figure 1b). By modifying the surface modification to selectively absorb target biochemical substances, this miniaturized system can wirelessly measure the viscosity of cerebrospinal fluid (CSF), intracranial pressure (ICP), and the glucose concentration in cerebrospinal fluid, and present the results in real-time on a mobile terminal. This system lays the foundation for long-term continuous monitoring of various signals related to health conditions. Through surface modification, it may also be extended to wireless sensing of numerous other biochemical substances and biomolecules. Beyond the implantable devices elaborated in detail previously, there exists a diverse range of implantable magnetic field sensors that operate on different principles [17–19].

2.1.2. Developing Technologies

The sensing technology that is currently under development: When conducting the monitoring of magnetic field signals within the human body, the most formidable challenges encountered are the extremely feeble field strength and the broad frequency range. The magnetic field strength spans from 10^{-10} T to 10^{-15} T, while the frequency range extends from a few hertz to several thousand hertz [20]. To address the issue of capturing weak magnetic field signals, researchers approach it from two perspectives: enhancing the sensitivity of magnetometers and developing advanced magnetic shielding materials.

- Superconducting Quantum Interference Devices (SQUIDs) [21] operate based on the principle of Josephson junctions. This technology is capable of detecting magnetic fields within the range of pT to fT [22,23]. Nevertheless, it has certain limitations. The most notable drawbacks include high costs, large size, and the necessity for cooling equipment and a shielding room [21,24,25]. Prior to system simplification and miniaturization, the application of this technology in implantable devices remains challenging. Despite these challenges, current research indicates that this technology holds great promise.
- Atomic magnetometers (AM): These devices heat atoms to elevated temperatures and utilize the pumping and detection mechanisms of an optical system to detect the magnetic decay of atomic spins [26,27]. Atomic magnetometers are further classified into two distinct types: optically pumped magnetometers (OPM) and spin-exchange relaxation-free magnetometers (SERF). Under specific conditions, the performance of atomic magnetometers can be on par with that of Superconducting Quantum Interference Device (SQUID) sensors. In particular, the atomic magnetometer operating on the SERF principle can attain a sensitivity of 10 fT/$\sqrt{}$Hz at 10 Hz [28,29]. One of the significant advantages of this sensing approach is that it does not necessitate any cooling structure. Consequently, its volume is substantially smaller than that of SQUIDs and can be fabricated to be just a few centimeters in size [30,31]. It holds the potential for transformation into an implantable device. Nevertheless, atomic magnetometers are not without their limitations. A fundamental drawback is that they can only function in an environment characterized by a near-zero magnetic field [27]. All varieties of atomic magnetometers necessitate magnetic shielding to maintain a near-zero ambient noise level in order to attain ultra-high sensitivity. Another shortcoming is that, owing to theoretical constraints, the bandwidth of atomic magnetometers is extremely narrow [32], which restricts the frequency range of bio-magnetic signals

that can be detected. Consequently, there remains a substantial distance to cover before atomic magnetometers can be put into practical use.

- Magnetic field shielding technologies (MSRs): Magnetic field shielding technologies play a crucial role in the magnetic field sensing system. The magnetic shielding room, as an essential component thereof, aims to mitigate background noise during the monitoring of bio magnetic fields. It can be classified into two categories: active and passive [30]. At present, research regarding magnetic shielding materials predominantly centers on the selection of materials for shielding rooms. A representative shielding material is the Mu material. This is a shielding material derived by incorporating various other components into a nickel-iron alloy as the base [33–35]. Moreover, novel materials such as manganese-zinc ferrite are under investigation as promising alternatives [36].

2.2. Piezoelectric Sensing

The piezoelectric effect stems from the linear electromechanical coupling between the mechanical and electrical states within crystalline materials lacking inversion symmetry. This effect is a reversible phenomenon: materials demonstrating the piezoelectric effect also manifest the reverse piezoelectric effect, wherein an applied electric field gives rise to the internal generation of a mechanical strain. The piezoelectric effect finds application in pressure sensing [37,38], whereas the inverse piezoelectric effect is frequently employed for the generation of ultrasonic waves. The advantages of this sensor lie in its ability to convert mechanical energy into electrical energy, thereby enabling self-power supply and eliminating the necessity for external power sources. Additionally, it features a simple structure and relatively high sensitivity. However, this type of device exhibits a greater sensitivity to dynamic signals and a lower sensitivity to static signals, which may impose certain limitations in long-term monitoring scenarios [39].

2.2.1. Applied Technologies

Polylactic acid (PLLA), a biodegradable polymer that finds extensive applications, also manifests certain piezoelectric properties upon appropriate treatment. This material exhibits shear piezoelectricity, which can be ascribed to the electrode polarity within the carbon-oxygen double bond branching from the polymer's main chain. By fabricating a 3 multi-layer structure, enhanced piezoelectricity can be attained from polylactic acid, and its "effective" conversion efficiency is comparable to that of ceramic PZT. Capitalizing on the favorable dielectric characteristics of polylactic acid, Curry developed a biodegradable piezoelectric polylactic acid pressure sensor [40]. The sensor was integrated with a charge amplifier circuit, a wireless near-field communication (NFC) chip, and a commercial antenna on a printed circuit board (PCB). The entire PCB was encapsulated within a polydimethylsiloxane (PDMS) box and implanted subcutaneously on the back of an animal, thus enabling implantable wireless sensing. The abdominal sensor and connecting wires are capable of self-degradation, while the non-degradable PCB can be easily removed through minimally invasive means at the end of the sensor's service life. Although PLLA has demonstrated remarkable potential in the realm of biodegradable piezoelectric materials and implantable sensors, other researchers are also exploring diverse materials to develop similar devices with distinctive advantages. For example, Yang reported a self-assembly method for wafer-scale synthesis of heterogeneous piezoelectric glycine thin films [41]. These films exhibit a PVA-glycine-PVA sandwich structure (Figure 1c). Glycine, the simplest amino acid, has a high piezoelectric coefficient and notable stability. The hydrogen bonds at the interface between PVA and glycine promote the formation and self-alignment of γ-glycine crystals across the entire film. The synthesized films display excellent, stable, and

uniform piezoelectric properties, along with remarkable flexibility and biocompatibility. The device can operate stably for 5 days and completely degrade within 10 weeks. This device can also be utilized for implantable respiratory measurement in mice. Nevertheless, the application of glycine films still encounters some challenges owing to their intrinsic properties. As a result, Chorsi proposed a different material processing strategy to tackle the brittleness and fragility of glycine films [42]. Polycaprolactone (PCL) was integrated into glycine crystals to fabricate biodegradable, flexible, and piezoelectric glycine crystal nanofibers (Figure 1d). The glycine-PCL nanofiber film demonstrates stable piezoelectric characteristics. Specifically, it exhibits a high ultrasonic output of 334 kPa at 0.15 volts root mean square (Vrms), outperforming existing biodegradable transducers. Biological experiments were conducted on mice, and the function of promoting brain drug delivery significantly extended the survival time of mice with orthotopic glioblastoma. Notwithstanding these progressions in material processing and device fabrication, the matter of wireless data transmission for implantable piezoelectric sensors remains a crucial factor to be taken into account for their practical applications. To achieve the wireless data transmission of implantable piezoelectric sensors, researchers at Purdue University designed an ultra-low power 2.4 GHz transmitter chip [43]. This chip was integrated with a patterned ring antenna on a flexible parylene C substrate. The ring antenna serves dual functions, acting as both a radiator and an inductor element within a voltage-controlled power oscillator (VCPO). Through this configuration, it achieves an ultra-high energy efficiency of 7 pJ/bit. The low-power active mode and sleep mode make it possible to implement continuous transmission and aggressive duty cycle data transmission. This advancement offers a practical solution for endowing the aforementioned biodegradable piezoelectric sensors with wireless functionality, thereby augmenting their overall practicality and applicability in biomedical domains.

2.2.2. Developing Technologies

In the realm of piezoelectric sensing, a number of novel technologies are currently in the process of development:

- Novel Forms of Piezoelectric Materials: Piezoelectric materials serve as the core constituents of piezoelectric sensors. The commonly utilized piezoelectric materials are classified into organic and inorganic piezoelectric materials. Organic materials typically exhibit excellent flexibility; however, their piezoelectric properties are generally inferior to those of inorganic piezoelectric materials. Researchers are delving into the manufacturing techniques of piezoelectric materials. By means of additive manufacturing and 3D printing technologies, piezoelectric ceramics, piezoelectric polymers, etc., can be fabricated into sensor components of appropriate geometries. For instance, piezoelectric thin films can be adhered to the surface or embedded within composite structures, departing from the conventional stacked wafer configuration [44].
- Distinct from the piezoelectric effect, which is exclusive to non-centrosymmetric materials, the flexoelectric effect represents an emerging area of research. It characterizes the coupling relationship between mechanical strain gradients and electrode polarization. The flexoelectric effect exhibits storage dependence, and this effect becomes more pronounced as the system size diminishes [45,46]. At present, investigations into flexoelectricity predominantly concentrate on principle exploration and the observation of the effect in crystals [47]. Researchers have developed curvature and torque sensors leveraging the flexoelectric effect [48,49]. However, there are no specific instances of its applications in the human body. There remains a vast expanse of research potential for flexoelectric effect sensors in biological tissues. Potential application scenarios

might encompass mass sensing, drug delivery, implantable micro energy storage devices, etc. [50–52].

- Piezoelectric Power Supply Network: Piezoelectric sensors, serving as an intermediary in the conversion of mechanical energy into electrical energy, hold the potential to power other implanted electronic devices. Nevertheless, currently, piezoelectric nanogenerators (PENG) are still confronted with issues such as low output power, unstable output, and a narrow frequency spectrum range. Ye enhanced the driving capacity of PENG via an improved LC matching network for frequency tracking and power regulation [53]. However, there remains a significant distance to cover before its practical application. Research indicates that resonance-based piezoelectric energy harvesters (PEHs) can amplify the resonance frequency. Nevertheless, this inevitably introduces the drawback of a narrow bandwidth [54], and simultaneously restricts the miniaturization of PEHs [55]. At present, no practical piezoelectric energy harvesting devices are available.

2.3. Capacitive Sensing and Inductive Sensing

As far back as 1967, Collins devised an inductance-capacitance (LC) passive wireless sensor. This sensor utilizes a spiral inductor linked to a sensing capacitor for the measurement of intraocular pressure. A readout coil is inductively coupled with the sensor to enable the wireless acquisition of sensor data. Minute disturbances cause alterations in the sensing capacitor, leading to a linear shift in its resonant frequency. Such wireless LC sensors have been further explored and applied for the monitoring of physical, chemical, or biological parameters [56,57]. Nevertheless, in applications like implantable, wearable, or other devices subject to geometric constraints, the reduction in the size of coils diminishes inductive coupling. Consequently, there is a pressing need to enhance the sensitivity of LC sensors. In recent years, researchers have employed a diverse range of methods to boost the sensor sensitivity.

The LC resonant pressure sensor relies on the sensitivity of capacitive/inductive components to the physical quantity under measurement. In an LC resonant circuit, alterations in the capacitance/inductance value lead to a change in the resonant frequency of the entire circuit. This variation can be detected by a coupled external inductive coil, causing a change in the impedance of the entire system, thereby achieving the conversion of the physical quantity into an electrical quantity. This approach obviates the need for active components, and passive operation does not necessitate a battery or an energy harvesting system. Depending on the distinct sensitive components, LC resonant sensors are classified into capacitive sensors and inductive sensors. This particular type of sensor features a simple structure and is amenable to straightforward manufacturing processes. Simultaneously, it exhibits a rapid dynamic response capacity, rendering it highly suitable for the real-time monitoring of rapidly fluctuating physiological signals. Incorporating an inductance coil within the sensor structure enables the implanted device to be powered via this configuration [58]. However, a notable drawback is that the stray capacitance within the lead cable and electronic circuit of the capacitive sensor can be substantially larger than the sensor's intrinsic capacitance, thereby diminishing the measurement accuracy [14].

2.3.1. Applied Technologies

Owing to the uncomplicated structure of the LC resonant circuit, researchers have conducted diverse optimizations on it. Dong-Yan Chen developed an inductor-capacitor passive wireless sensor featuring a nonlinear parity-time symmetric structure [59]. The quality factor of the LC passive wireless sensor with a PT symmetric structure, based on linear loss and saturated gain, was theoretically put forward and experimentally validated

to be improved. Under the small perturbation limit, the response singularity in this approach implies the enhancement of sensing performance (Figure 2a).

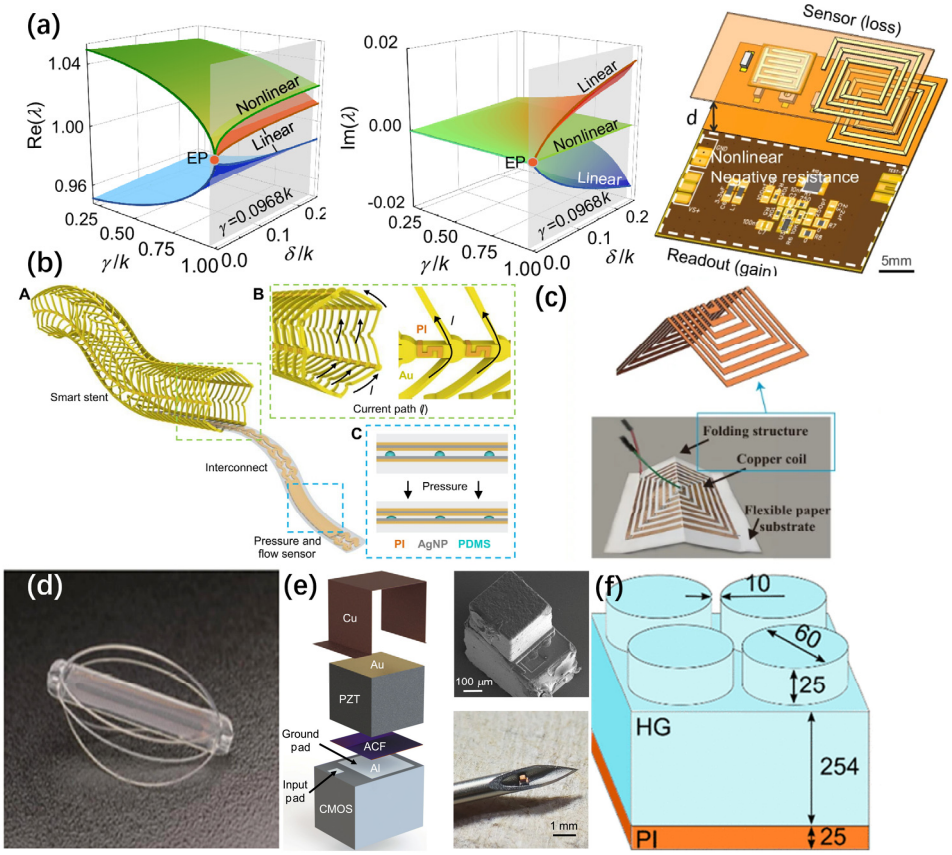


Figure 2. (**a**) Under different perturbations of nonlinear and linear systems, the functional relationships between the real and imaginary parts of the characteristic frequency and the coupling strength relative to the loss, as well as the wearable wireless LC sensor fabricated based on this principle. (**b**) In the design of the inductive bracket, a conductive Au ring and a non-conductive polyimide (PI) connector are used to achieve a solenoid-like current path and bracket structure. At the same time, a soft pressure sensor layer is constructed on its surface by means of a printed dielectric layer. In the third-level images, the inductive bracket design employs conductive Au rings and non-conductive polyimide connectors to realize a solenoid-like current path. Simultaneously, a printed dielectric layer is utilized to fabricate the soft pressure sensor layer. (**c**) The basic structure of PSIFS (**d**) The EndoSure sensor. (**e**) a deconstruction schematic diagram of the main components of the mote, which includes a CMOS temperature sensor chip with two exposed aluminum (Al) pads, a micro lead zirconate titanate (PZT) sensor coated with gold on both sides, an anisotropic conductive film (ACF), and a copper layer. This device can be implanted in the body with the help of a syringe. The presented content encompasses scanning electron microscope images of the microspheres. These microspheres exhibit a diameter of 300 μm, a length of 380 μm, a thickness of 570 μm (equivalent to a volume of 0.065 mm^3), and a weight of 0.3 mg. They are positioned at the tip of an 18 g needle, with an inner diameter of 0.84 mm and an outer diameter of 1.28 mm. (**f**) Design of the hydrogel-based structures used for implantation.

Furthermore, Wu conducted a structural design of the inductor within the resonant system [60]. A serpentine spiral structure inductor was employed. In contrast to the traditional spiral coil, the serpentine spiral coil offers lower radial stiffness. When the inductor is subjected to axial pressure, the spiral inductor undergoes axial compression. When the serpentine angle is zero, the inductor reverts to a traditional spiral inductor. Either increasing the distributed length or decreasing the cross-sectional area can reduce the inductance, thereby increasing the resonant frequency. Under the same axial load, the

more pronounced the change in the resonant frequency of the LC resonant sensor, the higher the sensitivity that the LC sensor can achieve.

The dimensions of implantable sensors and their compatibility with vascular surgical procedures have long imposed limitations on the morphological design of implantable devices. Herbert developed a three-dimensional sensor that circumferentially enwraps the exterior of arterial blood vessels [61]. A conductive loop, in conjunction with non-conductive connectors, forms a conductive pathway resembling a solenoid, which serves as an inductive antenna (Figure 2b). Simultaneously, multiple soft capacitive sensors are integrated onto the inner surface of the stent. This system facilitates the concurrent monitoring of pressure, pulse rate, and flow rate. Given that the stent is fabricated using femtosecond laser technology, it can undergo stretching and contraction to accommodate arterial blood vessels of diverse shapes, thereby demonstrating excellent versatility.

Beyond determining the configuration of the inductance coil, researchers are delving into multi-coil sensing systems. Silva employs a three—coil coupling system, composed of one implanted coil and two external coils [62]. The external coils are classified as a transmitting coil and a relay coil. The three—coil inductive link technology has the potential to optimize the readout system by leveraging the geometric characteristics of each coil and the distance between the transmitting coil and the relay coil. In this topological configuration, an increase in the mutual inductance between the transmitting coil and the relay coil is anticipated. This, in turn, will result in an augmentation of the mutual inductance between the readout coil and the implanted sensor. The enhanced mutual inductance can elevate the efficiency of the readout system in detecting the sensor. Experimental results demonstrate that when the distance between sensors in the readout system is zero, the relay sensor can function as a signal amplifier, thereby optimizing the detection of the sensor by the transmitting sensor.

Among the devices previously mentioned, several incorporate mutual inductance sensors as their fundamental components. A mutual inductance system necessitates a minimum of two distinct coils. To mitigate system complexity, Zhu employed an origami structure to fabricate a self-inductance sensor [63]. The key advantage of this sensor lies in the fact that it can fulfill its function with only a single coil, thereby reducing the complexity of the overall system. The substrate of this device is composed of ordinary paper material, on the surface of which a planar inductance coil is fabricated. When the paper undergoes bending, the deformation of the planar spiral coil in three-dimensional space can be exploited to measure angles (Figure 2c). The structural features of this sensor render it extremely suitable for measuring the flexion, extension, and rotation of human joints. Furthermore, the article conducted comprehensive mathematical calculations and electromagnetic simulations to identify the optimal structure of the inductance coil under the prerequisite of high sensitivity. These efforts provide a crucial design direction for future folded coils.

2.3.2. Developing Technologies

The dimensions and operating principle of LC resonant sensing impose limitations on its readout distance. As previously stated, relay coils are employed to strengthen magnetic field coupling and thereby extend the readout distance. This includes the enhanced cyclic scanning repeater and the adaptive repeater, as detailed in references [64,65]. Nevertheless, this approach gives rise to multiple peak frequencies in the spectrum and leads to a reduction in sensitivity. Recently, it has been discovered that the breaking of PT symmetry can contribute to an increase in the readout distance of LC sensors [66]. Moreover, it enables the achievement of a higher Q-factor [67] and simultaneous multi-parameter measurement [68]. However, there remain numerous controversies regarding the inevitable noise

and practical sensitivity of exceptional point sensors. The innovative construction strategy of PT sensors still necessitates further in-depth research and exploration [69]. Evidently, there is a substantial journey ahead before this technology can be effectively translated into practical applications. Furthermore, for resonant sensors, another crucial aspect is how to withstand environmental parameters and enhance sensitivity. LC passive sensors are more susceptible to environmental parameters (such as temperature and humidity) owing to the absence of active correction components. Moreover, the impact of noise on the signal is relatively significant [70]. To address this issue, several approaches have been put forward:

- Employing differential sensors to mitigate the environmental influence on the sensors via the superposition principle [71,72]. Nevertheless, this method imposes extremely high demands on the symmetry between the two resonators, posing a challenge during the sensor design and manufacturing processes [73].
- Augmenting the electric field surrounding the resonator serves to enhance the sensor's capacity to polarize molecules within the measured material, thereby boosting the sensor's sensitivity. This approach has been implemented in certain passive resonant sensors [74–76]. Nevertheless, in specific scenarios, noise sources in the environmental space can obscure readings featuring relatively minor frequency shifts. Consequently, the key challenge confronting this type of device remains how to mitigate environmental noise and further elevate the sensor's sensitivity [77]. There is an urgent need for the emergence of novel technologies.

In addition to the above research work, some companies have already developed commercial devices that can be used in surgeries. The EndoSure Sensor Wireless AAA pressure measurement system (CardioMEMS) (Figure 2d) that monitors blood pressure in an aneurysm sac is safe and useful in guiding endovascular repair of an abdominal aortic aneurysm (AAA) [78]. This research was published in the Journal of Vascular Surgery. Wireless implantable sensors can be used to diagnose the location and type of endoleaks during endovascular aneurysm repair. Compared with using contrast agent injection and X-ray imaging to monitor endoleaks, this method minimizes the damage to the human body during monitoring and avoids misdiagnosis caused by in vivo motion artifacts mimicking endoleaks.

2.4. Ultrasonic Sensing

The ultrasonic sensing principle of implantable sensor devices predominantly relies on the piezoelectric effect. Commonly employed piezoelectric materials include piezoelectric ceramics and piezoelectric polymers. When ultrasonic waves impinge upon piezoelectric materials, these materials generate electric charges as a result of mechanical stress, thereby efficiently converting ultrasonic signals into electrical signals. The converted electrical power can be harnessed to supply energy to the implantable system. Furthermore, by leveraging the reflection and scattering properties of ultrasonic waves, they can be utilized for wireless data transmission. Alternatively, through the analysis of the echo characteristics of implantable devices under diverse conditions using ultrasonic waves, the measured physical quantities can be derived. This distinctive feature renders it extensively applicable in the realm of biological signal detection. Implantable ultrasonic sensors possess distinctive advantages in medical monitoring. These include high sensitivity and non-contact measurement capabilities, enabling them to monitor in real-time the alterations in internal tissues [79]. Nevertheless, they are not without limitations. For instance, temperature fluctuations can undermine the measurement accuracy. Additionally, relatively large-sized ultrasonic transmitting and receiving devices are necessary, which poses challenges to the miniaturization of the system. Furthermore, the processing and reconstruction of ultrasonic signals remain highly challenging tasks.

2.4.1. Applied Technologies

The conversion of acoustic energy into electrical energy via piezoelectric transducers finds the most extensive applications. Chen et al. developed an ultra-tiny "particle" sensor integrated with a piezoelectric transducer [80]. This device features a size of less than 0.1 mm and a power consumption of less than 1 nW (Figure 2e). Through the monolithic integration of a customized low-power temperature sensor chip with a micro-piezoelectric transducer fabricated on top of the chip, the miniaturization of the volume was successfully achieved. The device volume is less than 0.1 mm^3, comparable to a grain of table salt. By reducing foreign body rejection and tissue damage, it enhances biocompatibility, enabling it to access narrower interstitial spaces and causing minimal interference to the physiological signals to be measured. Consequently, it can be implanted or injected using minimally invasive techniques with enhanced biocompatibility. This sensor can operate within the temperature range of 25 °C to 50 °C, which encompasses all relevant physiological temperatures. The average temperature error from 31 °C to 35 °C is approximately 0.044/−0.040 °C, and the maximum temperature error across the entire temperature range is approximately ±0.2 °C. In the scenario of multiple sensors implanted simultaneously, the spatial resolution can reach 10 μm. These data validate its effectiveness as a body temperature sensor.

Another application scheme for ultrasound is to utilize the resonant absorption of ultrasound by hydrogels. By design, the volume of the hydrogel can be made sensitive to certain physiological quantities. Corresponding changes in physiological quantities will cause the hydrogel to expand or contract, thereby altering its resonant characteristics. Nam introduced silica nanoparticles into the hydrogel network by loading, which increased the scattering of the propagating ultrasound [81]. The sensor operates in a differential mode, where two sound waves propagate through two different paths; one path contains the hydrogel loaded with silica, and the other path does not. Since the additional attenuation caused by the hydrogel, especially the embedded silica nanoparticles, varies with the volume change in the hydrogel. Therefore, the normalized ratio of the ultrasonic characteristics between the two interfaces is not affected by the changes in tissue characteristics and only depends on the response of the hydrogel to pH, thus making the output independent of the intermediate medium. To maintain the same functional relationship between the swelling behavior of the hydrogel and the pH value, the hydrogel was micropatterned to form a cube shape. A differential pulse echo measurement scheme was used to detect the volume response of the hydrogel. This ultrasonic hydrogel pH sensor successfully measured the pH value at a working distance of approximately 10 cm with a moderate sound intensity (<200 mW/cm^2). Within the range of the FDA's regulations for imaging ultrasonic intensity (720 mW/cm^2), using a higher ultrasonic intensity can extend the sensing distance. By replacing the hydrogel loading material, Navid Farhoudi embedded boronic acid groups into the hydrogel, forming a hydrophilic hydrogel network composed of acrylamide, methacrylate, and boronic acid components [82]. This network can produce a reversible volume response to glucose. The hydrogel is designed and shaped to exhibit a mechanical resonance frequency at a specific frequency while remaining acoustically transparent to other frequencies (Figure 2f). Therefore, conventional and continuous ultrasonic imaging can be performed. When tested in mice, during an implantation time of 6 h, the blood glucose was measured uninterruptedly every five minutes using an ultrasonic probe, and the system demonstrated good stability. The authors also conducted a detailed performance analysis of this system, which points the way for significantly enhancing the sensing performance characteristics.

2.4.2. Developing Technologies

One of the key challenges in ultrasonic sensing lies in the accurate reconstruction of ultrasonic signals into image signals. This is particularly pronounced in the case of implantable ultrasonic sensors. As their positions relative to the human body vary over time, ultrasonic images often suffer from distortion. Machine learning algorithms have been employed to rectify the image distortion induced by the displacement of ultrasonic transducers [83]. Nevertheless, this problem has not been fully resolved, and further investigation is still warranted.

Moreover, the disparity in elastic modulus between ultrasonic devices and human tissues represents another issue that demands attention. This mismatch can impede the smooth propagation of ultrasonic waves into human tissues. Currently, the prevalent approach is to utilize gels to form a coupling layer between the ultrasonic element and the skin. Acoustic gels and hydrogels are frequently utilized [84,85]. Nevertheless, after a certain period, these two types of gels tend to dry out and detach, rendering long-term medical detection unfeasible. Identifying a coupling material with optimal acoustic properties, long-term usability, and excellent adhesion and compatibility with both the skin and the transducer remains a significant challenge to be addressed in the field of ultrasonic sensing [86].

The table below comprehensively summarizes the detectable parameters and their corresponding performance of various sensing mechanisms. (Table 1.)

Table 1. Performance indicators of different sensors.

	Reference	Sensing Parameters	Sensing Performance
Magnetic field sensor	Miniature extravascular hall-based magnetic sensor [15]	Mean arterial pressure (ABP)	MAE less than 5 mmHg
	Millimeter-level magnetic implants [16]	Cerebrospinal fluid (CSF) viscosity, intracranial pressure and cerebrospinal fluid glucose level	Accuracy exceeds 95%
Piezoelectric sensor	Polylactic acid nanofiber film [40]	d_{33}	19 pC/N
	Glycine-PVA film [41]	d_{33}	6 pC/N
	Glycine-PCL nanofibers [42]	d_{33}	18.91 pC/N
Passive LC sensor	Nonlinear parity-time symmetric structure [59]	Temperature	resolution: 0.027 °C
	LC sensor with a new type of encapsulated helical coil [60]	Strain	MAE: 5.57%
	Wireless printing soft sensor [61]	Pressure	MAE < 1% Effective reading distances are 5.5 cm (in air) and 3.5 cm (in blood)
	Implantable sensor for abdominal aortic aneurysm [62]	Pressure	MAE < 10% Effective reading distance is 10 cm
	Paper-based self-sensing folding displacement sensor [63]	Displacement	Displacement resolution is 20 um Effective reading distance is 42.3 mm
Ultrasonic sensor	Hydrogel particles used for temperature monitoring [80]	Temperature	MAE is 0.044/−0.040 °C
	Hydrogel embedded with silica nanoparticles [81]	pH	The resolution is 0.2 pH unit variation, the effective reading distance is 10 cm
	Resonant hydrogel sensor [82]	Glucose	Accuracy $\geq$ 83%

3. Wireless Communication and Power Transmission

In implantable sensors, wireless data transmission and wireless power supply are two crucial modules, which exhibit both similarities and differences. Wireless data transmission serves to convey the physiological information collected by the sensor to external devices for real-time monitoring and analysis. Conversely, wireless charging is primarily concerned with providing continuous energy support to the sensor, thereby extending its service life and mitigating the inconvenience and potential risks associated with battery replacement. Both of these technologies rely on wave propagation for implementation. Certain technologies, such as electric field coupling, are capable of simultaneously performing wireless data transmission and wireless power supply, a concept known as simultaneous wireless information and power transfer (SWIPT). The two can operate within the same frequency band or different frequency bands and are regarded as a significant solution for the continuous communication of low-power devices and wireless sensors in the future Internet of Things. Distinct from traditional wireless information transmission and energy transmission systems, the SWIPT system must strike a balance between the communication rate and energy transmission efficiency to achieve optimal energy and information transfer [87]. This section predominantly delineates the common approaches to wireless data transmission and wireless power supply, elucidates their respective advantages and disadvantages, and presents several examples of commercial applications.

3.1. Wireless Information Transmission

Common data transmission methods for wireless implantable devices include Bluetooth, Radio Frequency Identification (RFID), Near Field Communication (NFC), ultrasonic waves, magnetic induction coupling, and more (for detailed data, refer to Table 2).

Table 2. Distances and rates of some wireless communication technologies.

Method	Range	Transfer Rate
Radio Frequency	100 m	1–10 kbps
Bluetooth	10 m	1 Mbps
Near Field Communication	4–20 cm	106–424 kbps

Bluetooth: Bluetooth communication is commonly seen in mobile phones and wearable electronic devices (such as bracelets and smart watches). It possesses several advantages, including low power consumption, user—friendliness, and high data transmission efficiency. However, the typical communication frequency band of Bluetooth is 2.4 GHz, which is susceptible to interference from wireless devices such as WIFI, smartphones, or microwave ovens. After years of development, BLE (Bluetooth Low Energy) has been developed specifically for low-power devices. It reduces the energy consumed in data transmission and extends the usage time of implantable devices [88]. At present, the commercially available Eversense E3 continuous glucose monitoring system is implanted beneath the patient's skin to monitor the glucose content in subcutaneous fluid. A wireless transmitter worn externally on the patient's body acquires information from the sensor and transmits glucose readings to the user's mobile device via Bluetooth every five minutes [89]. The Nalu Neurostimulation System developed by another company involves the implantation of a micro-stimulator under the skin. This system utilizes gentle electrical pulses to block pain signals prior to reaching the brain, offering a drug-free therapeutic approach. It enables wireless control through Bluetooth Low Energy technology. Patients can utilize a smartphone remote control application to select treatment options and regulate the stimulation, while doctors can also perform remote management via a clinical programming application [90].

Radio Frequency Identification: RFID is a better choice when it is difficult to power the object to be identified. RFID tags can work without a power source. They obtain energy from the reader, require no physical contact, and the wireless reading distance is relatively compatible with the depth of implantable devices [91]. Simultaneously, RFID technology is capable of concurrently reading the information of multiple sensors without interference, rendering it suitable for the simultaneous implantation of multiple sensors. Nevertheless, this technology does have certain limitations. High-frequency RF signals, such as those at 2.45 GHz, exhibit substantial scattering and absorption within the human body. For an antenna designed for external radiation, the calculated maximum Specific Absorption Rate (SAR) value at 2.45 GHz is 0.0369 W/kg. When an antenna designed for in-body communication is employed, the maximum SAR value at the same frequency escalates to 0.4479 W/kg. The significantly elevated SAR value of the antenna during in-body transmission poses certain challenges to signal reading [92]. Moreover, owing to the absence of unified RFID standards, issues regarding system interoperability among different suppliers exist. Seamless integration with existing systems is arduous, and there is also a risk of data leakage. In the commercial domain, RFID finds extensive applications. The Raumedic intracranial pressure sensor, a precision measurement catheter employed in the neurosurgical domain, is primarily utilized for monitoring parameters including intracranial pressure (ICP), temperature, and partial pressure of oxygen. By leveraging technologies such as semiconductor pressure sensors and thermistors, it enables direct and accurate in situ measurement of intracranial pressure. The measurement data is transmitted to the patient monitor via RFID technology [93]. Medtronic's Chronicle, an implantable hemodynamic monitor, integrates cardiac electrophysiological monitoring with a right ventricular pressure sensor. This device aids doctors in managing heart failure patients by closely monitoring heart function and pressure variations [94]. VeriChip Corporation has developed an implantable RFID tag that can be implanted in the upper arm. By transmitting a unique serial number, it facilitates medical professionals in swiftly retrieving the patient's medical information. Even when the patient is unconscious or unresponsive during surgery, doctors can precisely obtain the necessary information.

Near Field Communication: NFC provides high-speed data transmission over short distances. This transmission method has high security and can protect user privacy well. However, its effective distance is short, and it is only suitable for body surface sensors [95]. Simultaneously, when dealing with scenarios that demand high-capacity data transmission, the transmission rate of NFC often falls short of meeting the requirements. Implantable sensors leveraging near-field communication have been successfully developed [96]. These sensors can effectively address the issue of implantable sensors relying on battery power. Moreover, several commercial sensors operating on this principle have already found practical applications. For instance, the flexible NFC skin tags developed by Gentag are capable of monitoring patients' activities and vital signs. They can transmit the collected data to external devices via NFC technology. These tags utilize a flexible polymer substrate and are attached to the skin for non-invasive biophysical measurements. The data is then collected using smartphones [97].

Magnetic Induction Coupling: This transmission method is grounded in the principle of electromagnetic field resonance. The implanted component therein is, in fact, a resonator. The characteristics of the implanted resonator undergo changes in accordance with the variation in the target signal, thereby generating a signal that can be remotely measured. The parameter to be measured is traced by gauging the alteration in the resonance frequency [98]. Typically, passive transmission sensors can be classified into LC resonators, radiofrequency cavity types, patch antenna types, surface acoustic wave (SAW) types, etc. [99–101]. The merits of this wireless communication mode include the absence of a re-

quirement for an implanted battery, a simple structure, a compact volume, and convenience for mass production. Nevertheless, a drawback is that the reading accuracy is significantly influenced by environmental factors (such as motion interference and electromagnetic interference). Also, during the reading process, the sensor and the reader must maintain a fixed distance and a specific alignment method; otherwise, the detection results will be compromised [102]. Furthermore, the effective transmission distance of electromagnetic coupling is restricted, and a small distance needs to be maintained between the reading device and the sensor [56]. Furthermore, when multiple sensors communicate concurrently, electromagnetic field interference will arise, leading to the inability of reading the data of a single tag. Special coding or modulation techniques are thus necessary to address this issue [103]. In the commercial domain, passive transmission sensors are also extensively employed in disease monitoring and prevention. The first human implantable inferior vena cava (IVC) sensor, FUTURE-HF, can be utilized for the surveillance of cardiovascular diseases like heart failure. Its volume measurement exhibits a high degree of consistency with the CT results (R2 = 0.98). A 6-month follow-up reveals that NT-proBNP has significantly decreased (p = 0.026) and heart failure events are reduced by 80.3%, offering precise technical support for remote congestion management [104]. Simultaneously, CardioMEMS EndoSensor™, recognized as the smallest wireless implantable blood pressure sensor available on the market, is specifically designed for monitoring the blood pressure of patients with cardiovascular diseases (including heart failure, abdominal aortic aneurysm, and hypertension). This device is implanted outside the vascular repair site, with a volume of approximately 0.23 cubic centimeters. It does not necessitate electronic components or batteries and has a service life of over 3 years [78].

Ultrasonic Waves: Different from the previous four communication methods, this method transmits information through the vibration of sound waves. Ultrasonic waves have good penetration in the human body. Using this method, sensors can be placed deeper in the human body to obtain physiological data that is difficult to detect by other methods. Medical ultrasonic equipment has found extensive applications. Ultrasonic imaging devices, including B-mode ultrasound and color Doppler ultrasound, are capable of clearly depicting the internal structure and tissues of the human body, thereby facilitating physicians in disease diagnosis. Ultrasonic diagnostic equipment, employed in cardiac ultrasound, vascular ultrasound and other examinations, can detect internal lesions and anomalies within the human body. Nevertheless, at present, there is a dearth of commercial ultrasonic communication sensors for implantable devices. This represents an issue that demands resolution and can be regarded as a potential research avenue in the future.

3.2. Wireless Charge

Inductive coupling: Energy is transferred to implantable medical devices, including cardiac pacemakers, defibrillators, neuromuscular stimulators, etc., via inductive coupling. Lyu et al. designed a compact stimulator with dimensions of merely 5 mm × 7.5 mm [105]. Operating at a resonant frequency of 198 MHz, it can be positioned up to 14 cm away from the external transmitter and stores energy through a switched capacitor. Once the voltage reaches the threshold, the stored energy is released as a stimulation output. By employing a positive feedback trigger circuit, the requirement for a stimulation control circuit block is eliminated, thereby saving valuable space. In the in vivo experiment, two electromyogram (EMG) recording electrodes were implanted into the gastrocnemius muscle of rats, while the ground electrode was attached to the skin, successfully demonstrating the functionality of the stimulator.

Magnetic resonance coupling: Magnetic resonance coupling realizes energy transmission through transmitting and receiving resonators, featuring high efficiency and rel-

atively long transmission distances. Li proposed a wireless magnetic resonance energy transmission system for miniature implantable medical sensors [106], achieving efficient, stable, and lossless energy transmission (Figure 3a). Through experiments, it was verified that this system exhibits good performance and stability under different distance and load conditions.

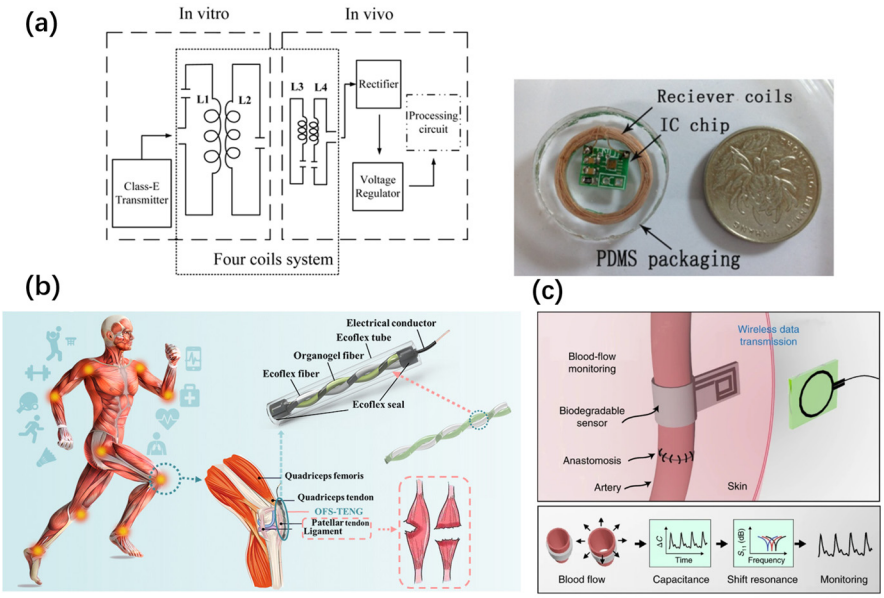


Figure 3. (**a**) Schematic diagram of the wireless resonant energy transmission system and the implanted receiver coil and IC chip packaged in PDMS. (**b**) Application and architecture of the OFS-TENG. (**c**) Capacitive pulse sensors installed around the arteries measure the changes in vascular diameter caused by arterial pulsation. The change in capacitance causes the resonant frequency of the LCR circuit to shift. This change was measured by the external reading coil.

Ultrasonic transmission: Ultrasonic waves achieve energy transfer by means of sound waves. Given that biological tissues have a relatively low absorption rate of ultrasonic waves, this characteristic gives it distinct advantages in energy transmission for tiny implants or deep tissues. For example, Kim et al. developed an implantable pressure sensing system driven by mechanical vibration [107]. This system utilizes the piezoelectric effect and can collect ultrasonic energy with a great power density. Specifically, it converts acoustic vibration harmonics into electrical energy and then charges a capacitor. During the period when the cantilever beam is in a non-vibrating state, the stored charge is discharged through an LC resonant circuit equipped with a pressure-sensitive inductor, providing the required energy for deep brain stimulation.

Triboelectric nanogenerator: Leveraging the triboelectric effect, it is capable of converting the mechanical energy within the human body into electrical energy, thereby endowing devices with the self-power supply capacity. As the pioneer of the triboelectric nanogenerator, Wang put forward a self-powered implantable ligament strain sensor grounded in triboelectric nanogenerator technology [108]. Powered by the triboelectric nanogenerator, upon being implanted into the patellar ligament, this sensor can generate electrical signals during human locomotion. These signals are utilized to assess the damage of muscles or ligaments (Figure 3b). Furthermore, this implant elicits only a mild inflammatory response.

Table 3 lists the power, distance and size of different wireless charging solutions.

Table 3. Different types of wireless charging data.

Reference	Transmission Power	Energy Transmission Distance	Size
Inductive coupled stimulator [105]	>2.7 μW	14 cm	5 mm × 7.5 mm
Wireless magnetic resonance energy transmission system [106]	At a distance of 2 cm, the received voltage signal is converted into a stable 3.3 V output voltage and a current of 10 mA.	1–3 cm	The diameter of the receiving coil is 1.9 cm
Ultrasonic piezoelectric transducer [107]	16 mW	10 cm	40 mm × 8 mm
Triboelectric nanogenerator [108]	Maximum 0.7 V (150% stretching)	N/A	6 cm

3.3. Antenna Design

This section presents the antenna of implantable devices. The antenna serves as the physical foundation for both wireless data transmission and power transmission, being capable of receiving and transmitting signals. Implantable antennas are thus required to possess characteristics such as compact size, low power consumption, and robust anti-interference capabilities. Simultaneously, biocompatibility must be taken into consideration. Implantable antennas should prevent short circuits and the generation of harmful radiation to surrounding tissues to safeguard the health of patients. Consequently, medical antennas are confined to a specified frequency range [109]. Commonly employed implantable antenna structures encompass helical/meandering antennas, planar inverted F antennas (PIFA), and conformal antennas. In recent years, the key innovation aspects have predominantly centered around multi-band applications, reconfigurable features, novel materials, and manufacturing processes, among others.

Spiral antenna: The helical antenna offers the advantage of a small volume. The polarization field it generates is circular, and it exhibits the characteristic of omnidirectional radiation. With relatively low requirements for directivity, it is well-suited for implantable devices. In 2019, Tutku Karacolak put forward an implantable antenna for continuous glucose monitoring, which operates in the Medical Implant Communication Service (MICS) (402–405 MHz) and Industrial, Scientific, and Medical (ISM) (2.4–2.48 GHz) frequency bands. The antenna was optimized for the dual frequency bands. The dual-frequency design enables the implant to switch between sleep and wake-up modes, thereby conserving energy and prolonging the service life of the implant [110] (for detailed data, refer to Table 4).

Simultaneously, with the advent of 3D printing technology, it has become possible to fabricate novel antennas with intricate shapes. In 2020, Youssef Tawk proposed a new type of 3D printed double-cone nested antenna. This antenna is composed of two conical spiral arms that are intertwined and oriented in opposite directions to implement an orthogonal circular polarization scheme. The nested conical spiral is manufactured through 3D laser printing and copper plating processes. The outer spiral arm is designed to resonate at 2.4 GHz, while the inner arm is intended for operation at 5.4 GHz. The entire antenna structure is arranged in an array, and its lattice can be dynamically altered between linear or triangular topological structures to reconfigure the radiation pattern [111]. Meanwhile, some researchers are dedicated to the optimization of antenna structures. Among them, Lamkaddem developed a circularly polarized miniaturized implantable antenna specifically designed for wireless cardiac pacemakers [112]. The circular polarization characteristic endows this antenna with unique advantages, enabling it to maintain reliable

communication with external devices in different orientations and effectively reducing the influence of human multipath reflections. This antenna achieves the goal of miniaturization through a meandering line design and ensures the performance of the circularly polarized antenna by adopting a U-shaped structure.

Table 4. Parameters of different types of antennas.

Reference	Frequency Band	Energy/Bandwidth	Size
Dual-frequency implantable antenna [110]	402–405 MHz/ 2.4–2.48 GHz	The bandwidth of the −10 dB bandwidth MICS band is 35.3%, and the bandwidth of the ISM band is 7.1%	22.5 mm × 22.5 mm × 2.5 mm
Double-cone nested antenna [111]	2.4 GHz (Outer arm) 5.4 GHz (Inner arm)	The peak gain of the external component is 9.8 decibels at 2.4 GHz, while that of the internal component is 7.8 decibels at 5.4 GHz.	Diameter: 4 cm
Circularly polarized small antenna [112]	915 MHz	With an impedance bandwidth of 18.9% in the 810 to 980 MHz band and an axial ratio of 17.2% in the 850 to 1010 MHz band, the gain value is −23 dBi.	5.2 mm × 5.6 mm × 0.25 mm
PIFA for polarization reconfigurability [113]	2.45-GHz ISM band	The measured bandwidths were 11.3% (2.26–2.53 GHz) and 9.1% (2.3–2.52 GHz), respectively, and the measured gains were −24.5 and −24.2 dBi, respectively.	13.5 mm × 11.5 mm × 1.905 mm
Microstrip technology PIFA [114]	402 MHz	The bandwidth is 39 MHz, the gain is −24.31 decibels, and the radiation efficiency is 8.72%	12 mm × 12 mm × 1.9 mm
Conformal antenna [115]	2.45 GHz	With a bandwidth of −10 dB and 280 MHz, at 2.45 GHZ, the antenna reflection coefficient is −14 decibels and the peak gain is −19.6 decibels	6 mm × 5 mm

Inverted F Antenna (PIFA): The device features a relatively compact size. The radiation pattern and input impedance can be accurately tuned by means of designing the pointing direction and feeding position, enabling personalized adjustment. Xian-Tao Yang put forward the first implantable antenna with polarization reconfigurability. By employing two sets of PIN diodes as RF switches, it is capable of switching between two orthogonal linear polarizations, thereby preventing communication link failures and demonstrating excellent robustness in complex implantation scenarios. In vitro experiments were carried out in a tissue-mimicking liquid. Under different reconfigurable states, the overlapping impedance bandwidth ranging from 2.3 GHz to 2.52 GHz is 9.1% [113]. In demanding implantation environments like retinal surgery, Hans Permana designed a three-layer PIFA antenna based on microstrip technology. Through its compact size design, its perfor-

mance surpasses that of other previously proposed implantable antennas, with a gain of −24.31 dB and a radiation efficiency of 8.72% [114].

Coupled antenna: A typical planar LCR resonator is composed of a capacitor in series with a planar coil. An additional manufacturing step is required to establish the electrical connection between the inductor and the capacitor. Boutry designed a dual-inductor coil structure [115]. In this structure, two coils are simply stacked, and a 50-micron-thick polylactic acid (PLLA) layer is used as an insulating medium in the middle (Figure 3c). This design does not require any additional electrical connections. It achieves the separation of the position of the pressure-sensitive area and the position of the wireless connection, significantly reduces the complexity of sensor manufacturing, and improves the overall stability of the device at the same time.

Conformal antenna: Conformal antennas possess the ability to adapt to the geometries of complex implantation sites and are well-suited for placement on the surfaces of irregularly shaped objects, such as organ tissues. Khan employed a method that combines a miniature coplanar implanted antenna with a sensor module, which can be utilized for intracranial pressure monitoring. The recorded intracranial pressure is transmitted to the skull, and a link budget within the range of 0.5–1 m is established. This constitutes an integral part of the minimally invasive intracranial pressure monitoring technology. Intracranial pressure is monitored at 2.45 GHz by means of a circular slot antenna. The radiation efficiency of this antenna outperforms that of previously utilized strip antennas, such as the printed inverted F antenna [116]. In the research of conformal metasurfaces, there are also crucial aspects deserving attention. Soumyadeep Das designed a conformal absorber metasurface to decrease the specific absorption rate (SAR) of implanted antennas. Reducing the SAR of implanted antennas is one of the significant design considerations in modern healthcare applications. The introduction of an absorber metasurface can restrict the backward radiation of the antenna, thereby regulating the SAR value. This technology reduces the maximum SAR value by 24% and significantly diminishes the average SAR distribution, thus alleviating the harm of electromagnetic radiation to human health [117].

Other antenna types: Malik, on the other hand, conducted an in-depth analysis of various types of antennas, such as planar antennas, wired antennas, conformal antennas, and spiral antennas, and elaborated in detail on the requirements and challenges faced by these different types of antennas [58]. Based on the specific requirements for implantable antennas in practical applications, he innovatively proposed a design scheme for a slotted patch antenna. In this scheme, both the substrate and the superstrate are made of Rogers RT6010 material. This patch antenna has the remarkable advantages of tiny size and easy integration. It has a wide radiation pattern and excellent frequency band characteristics, fully demonstrating the great application potential of patch antennas in the field of implantable electronic devices.

All the implantable sensors of various types mentioned above must be extracted from the human body via minimally invasive surgery and other techniques once the preset monitoring period is concluded. This procedure will inevitably inflict damage on patients. Particularly when surgeries are carried out in certain critical areas (such as the brain, arterial blood vessels, etc.), it will bring about unpredictable risks. In light of this, biodegradable electronic devices have already emerged as the development trend of implantable medical electronic devices. The latter part of this article will present the material selection and development status of biodegradable electronic devices.

4. Degradable Sensor Materials

Implant materials, which are required to remain within the human body for an extended period, must exhibit biocompatibility with the recipient's body. In accordance

with the international standard ISO 10993 [118], medical devices implanted in the human body are obligated to undergo biological evaluation. The objective of this evaluation is to ensure that the implanted device will not inflict harm on the human body. This comprehensive evaluation encompasses the assessment of the physical and chemical properties of the product materials. More specifically, it involves evaluating the compatibility of the mechanical parameters of the implant material with the surrounding human tissues and determining whether its chemical composition will trigger harmful reactions, such as tissue inflammation. Additionally, toxicological evaluation is an integral part of this process, aiming to investigate whether the material and its degradation products are toxic or carcinogenic. Moreover, the degradation characteristics of the implant material are of utmost importance. Under the environmental conditions of the implantation site, including specific temperature, pressure, and chemical composition, it is essential to examine whether the degradation rate of the implanted device aligns with the design requirements.

The criteria for implantable materials expounded in this article are grounded in the standards promulgated by the International Organization for Standardization, rather than the mandatory standards of any specific country or region. These criteria function as an auxiliary instrument to assist researchers in material selection.

The ISO 10993 standard defines an implantable medical device as one that is anticipated to be completely introduced into the human body or replace the epithelial or ocular surface via clinical intervention and is expected to remain in position following implantation. Materials implanted in the human body must undergo a variety of tests stipulated by ISO 10993. The objective is to safeguard humans from potential biological hazards associated with the utilization of medical devices. The test items typically encompassed in this standard include vitro cytotoxicity tests, skin irritation tests, sensitization tests, and so on.

Cytotoxicity: Cytotoxicity experiments employing cell culture techniques can be utilized to ascertain cell death, cell growth inhibition, colony formation, and other cellular responses induced by medical devices, materials, and their extracts.

Sensitization test: The sensitization experiment serves to assess the potential contact sensitization reactions of medical devices, materials, and their extracts. This experiment is indispensable as even minute amounts of potential leachable substances can trigger sensitization, thereby leading to allergic reactions.

Skin Irritation (Including Intradermal Reaction): The irritation assay serves to quantify the potential irritating impacts of medical devices, materials, and their extracts at relevant sites. The intradermal reaction assay is employed to assess the local tissue response to the extracts of medical devices. Additionally, the intradermal reaction can be applied to medical devices that are not amenable to skin or mucosal irritation testing (such as the implantable medical devices addressed in this article).

Blood Compatibility: The blood compatibility assay is designed to evaluate the effects of medical devices or materials in contact with blood on blood or its components.

Acute/Chronic Toxicity: In cases where there is a potential for the absorption of toxic leachable substances and degradation products, the acute toxicity experiment serves as a valuable tool to assess the potential hazards associated with an animal model's exposure to medical devices, materials, and their extracts either once or multiple times within a 24 h period. This experimental approach provides insights into the immediate effects of such exposures. On the other hand, the chronic toxicity experiment is designed to measure the impacts of exposure to medical devices, materials, and their extracts, which may occur either once or repeatedly over at least the majority of the experimental animal's lifespan. This long-term assessment helps in understanding the cumulative and delayed effects of these exposures.

Implantation Reaction: The implantation experiment is employed to evaluate the local pathological effects of an implant on living tissues through both macroscopic and microscopic examinations. To conduct this experiment, the medical device is surgically implanted into a pre-determined site or tissue. It is crucial that the experimental time and route of exposure closely mimic those of the actual medical device or material, ensuring the relevance and accuracy of the results obtained.

Degradation: For medical devices engineered to be absorbable, degradation experiments are essential. These experiments aim to comprehensively describe the mechanism of biodegradation, precisely determine the potential degradation rate, and identify the release of any potential toxic chemical substances. Depending on the specific requirements of the device, in vivo degradation experiments may be necessary to provide a more realistic assessment of the degradation process within a biological system.

In the realm of practical medical and healthcare, biodegradable materials exhibit distinct advantages that traditional materials lack. For instance, biodegradable implants gradually undergo degradation and are assimilated by the human body subsequent to fulfilling their medical functions. This obviates the necessity for a secondary surgical procedure for removal, thereby alleviating the patient's pain and reducing medical expenses. Simultaneously, these materials demonstrate excellent biocompatibility, enabling them to coexist in harmony with human tissues. This effectively mitigates rejection reactions and inflammation. Post-usage, they can degrade spontaneously, minimizing long-term environmental contamination and the burden associated with medical waste disposal. In certain specific scenarios, biodegradable materials can also offer transient support for tissue regeneration. As the tissue recuperates, these materials gradually degrade, creating room for the growth of fresh tissue, which is conducive to tissue repair and regeneration. Nevertheless, these materials are not without certain limitations. For example, in comparison with traditional materials, biodegradable materials exhibit relatively inferior mechanical properties, and these properties tend to deteriorate more over time. When the device is required to be utilized for a specific duration or degrade at a specified rate, it is essential to meticulously design the composition and structure of the biodegradable material to fulfill the usage requirements. Even though the degradation products are non-toxic to the human body, they may still impact the physiological functions of local tissues.

The degradable materials presented in this article are primarily classified into three categories: degradable metal materials, degradable silicon-based materials, and degradable polymer materials.

4.1. Degradable Metallic Materials

Currently, the metals frequently employed in implantable devices predominantly encompass traditional metal materials such as magnesium and its alloys, zinc and its alloys, molybdenum metal, and iron. Their degradation rates exhibit variations (for detailed data, refer to Table 5). Among these, magnesium demonstrates excellent biocompatibility and the most rapid degradation rate; zinc possesses moderate mechanical strength and degradation rate, and its decomposition products are non-toxic; molybdenum features high mechanical strength and good corrosion resistance. However, the limitation is that its degradation rate is slow, rendering it inappropriate for transient electronic devices; iron has the lowest cost, good biocompatibility and mechanical properties, and its metabolic pathway within the human body is clearly controllable. At present, medical biodegradable metal materials are primarily applied in domains such as nerve implant devices [119,120], vascular stents [121,122], and orthopedic implants [123,124].

Mg: Magnesium and its alloys have an elastic modulus similar to that of human bone tissue and are widely used in the field of orthopedic repair. In terms of electronic devices, magnesium metal is often used to manufacture key components of sensors due to its high electrical conductivity and ease of processing and decomposition. For example, it is used in power receivers and miniature heaters of implantable medical devices. Rüegg successfully prepared a magnesium-based radiofrequency degradable micro resonator [125]. This resonator can achieve frequency-selective wireless heating. This achievement marks an important step forward in using magnesium and its alloys as electrical receivers and miniature heaters in biodegradable implantable medical devices. Meanwhile, magnesium is also commonly used in the manufacturing of radio frequency coils and antennas for passive sensors. Wireless information transmission is achieved through the physical field coupling between the coils [126].

Zn: Zinc and its alloys have good biocompatibility and biodegradability. After special treatment, the strength level of zinc alloy implants is almost twice that of magnesium alloys [127]. Moreover, zinc batteries have advantages such as high safety, low cost, and relatively high energy density, making them suitable for the energy storage systems of implantable electronic devices. For example, an implantable zinc-ion battery based on a gelatin/polycaprolactone composite gel electrolyte completely degrades within 8 weeks in rats [128].

Fe: Ferroelectric materials hold significant promise for crucial applications in implantable electronic devices owing to their outstanding piezoelectric properties. Zhang et al. developed a biodegradable organic small-molecule ferroelectric crystal that demonstrates a piezoelectric response (with d33 reaching 138 pC/N), comparable to that of inorganic barium titanate ceramics [129]. This material can be utilized to fabricate flexible ferroelectric composite films for the assembly of controllable transient electromechanical devices.

Mo: As one of the bioabsorbable metals, molybdenum is widely used in the fabrication of electrodes for implantable electronic devices and energy devices. Molybdenum has good biocompatibility and can gradually degrade in biological fluids, making it suitable for short-term implantable electronic devices. Sheng proposed a high-performance, fully biodegradable and bioabsorbable supercapacitor implant using two-dimensional amorphous molybdenum oxide (MoOx) flakes as electrodes [130]. The research team further proposed a high-performance biodegradable energy storage device realized by a MoO_3-MoS_2 nanosheet array based on a two-dimensional heterostructure [131]. This device exhibits excellent performance in air/liquid environments, capable of providing a stable high output voltage (about 1.6 V) and a relatively long working lifespan.

Table 5. The degradation rates of various metals within the human body environment.

Metal	Degradation Rate	Degradation Product
Mg	In Hank's solution, the degradation rate of magnesium is approximately 0.35 mm/year, as reported in reference [132].	$Mg(OH)_2$, H_2
Mo	In the simulated physiological solution (c-sbf-ca, pH = 7.4), the corrosion rate of pure molybdenum is approximately 10 μm/year, as presented in reference [133].	H_2MoO_4
Fe	Pure iron was immersed in the simulated body fluid (SBF) solution, and the mass loss was measured. The response of human endothelial cells (EC) to various concentrations of ferrous ions was investigated via the WST-8 assay. The results indicated that the average in vitro degradation rate of iron is approximately 20.4 μg/(cm^2·h), as described in reference [134].	Fe_2O_3, Fe_3O_4
Zn	The corrosion rate of pure zinc in the simulated body fluid is approximately 0.02 mm/year, as shown in reference [135].	$Zn(OH)_2$, ZnO, $ZnCO_3$

4.2. Silicon-Based Materials

Degradable silicon-based materials are generally classified into ultra-thin silicon, silica gel, and amorphous silica. These three materials are all considered to be non-toxic and harmless to the human body.

Under normal circumstances, silicon is typically considered a material that is inherently resistant to natural degradation, with its degradation process often spanning hundreds of years. Nevertheless, silicon thin films can undergo decomposition within a time frame that, despite appearing relatively slow, remains within an acceptable range. The decomposition rate is approximately 5–90 nanometers per day [136]. Simultaneously, by introducing impurities into silicon through doping and depositing an oxide layer on the exposed surface, the time scale of this dissolution process can be precisely regulated [137]. When silicon dissolves in water, it engages in a chemical reaction with water to form silicic acid. Furthermore, the ultra-thin silicon surface can be fabricated by means of well-established microfabrication techniques. Owing to these merits, it holds significant application potential in the domains of biomedical implants and environmental monitoring. Nevertheless, ultra-thin silicon still presents several drawbacks that remain unresolved for the time being. For instance, ultra-thin silicon is relatively fragile and might cause harm to the human body upon decomposition. Additionally, the production cost of ultra-thin silicon wafers with a thickness below a certain threshold is relatively high, which is unfavorable for large-scale commercialization.

Eye Sensor: Yuting Shao fabricated a flexible and biocompatible multifunctional smart contact lens (P&T@DG) using flexible transfer printing and micro/nano processing technologies. This lens is based on an ultrathin single-crystalline silicon nanomembrane with a thickness of 200 nm. It can rapidly and accurately capture intraocular pressure (IOP) fluctuations and monitor ocular surface temperature (OST), thereby being applicable for multi-dimensional auxiliary diagnosis of glaucoma [138].

Electroencephalogram Interface: Mengge Wu developed a flexible transfer technique for single-crystalline silicon nanomembranes and subsequently established tens of thousands of implantable large-scale flexible electrode arrays with a controllable distribution density across the entire brain dimension (exceeding 32,000 electrodes). These arrays can adhere seamlessly to the cerebral cortex, reducing interface impedance and motion artifacts. They are capable of mapping real-time neural signals with high fidelity, achieving a high spatio-temporal resolution of 1.42 milliseconds and 20 μm, along with a signal-to-noise ratio of up to 37 decibels [139].

Silicone is a substance that exhibits extremely low decomposition rate over time, rendering it non-degradable within the human body. Nevertheless, its favorable physical and chemical properties, along with remarkable biocompatibility, have led to its extensive utilization in the medical domain. Silicone demonstrates a broad spectrum of hardness levels, outstanding anti-ultraviolet capabilities, excellent heat resistance, and chemical inertness. Moreover, it possesses superior electrical properties and can be effectively sterilized through various methods. Ranging from wound care gels to flexible drainage tubes and semi-rigid implants, silicone is prevalent in medical device applications [140–144].

Amorphous silicon: Amorphous silicon is a silicon structure characterized by long-range disorder and functions as a direct-band semiconductor. It offers distinct advantages, including straightforward production processes and relatively low costs. Nevertheless, it also presents several notable drawbacks. Specifically, the carrier mobility and minority carrier lifetime of amorphous silicon are significantly lower compared to those of single-crystalline silicon. Moreover, its performance is highly susceptible to degradation under illumination and high-temperature conditions.

Notwithstanding these limitations, when employed as the foundation for degradable devices, these disadvantages can be mitigated to a certain degree. Huang et al. developed an insertable, fully degradable optoelectronic cardiac pacemaker based on amorphous silicon. By depositing amorphous silicon optoelectronic units onto degradable metal wires, they successfully achieved the self-powered pacing function of the heart [145]. Hu Tao et al. realized a self-powered and conformal-contact cardiac pacemaker through the construction of hydrogenated amorphous silicon radial junction optoelectronic units [146]. Furthermore, amorphous silicon finds extensive applications in various other flexible electronic devices and demonstrates great potential in the fields of biodegradable electronics and green electronics [147].

4.3. Degradable Polymeric Materials

The commonly used biodegradable polymer materials for implantable biodegradable electronic devices mainly include the following types: 1. Polymers and copolymers; 2. polysaccharide materials; 3. Biomass materials, organometallic materials, etc.

- Polymers and copolymers:

Polylactic acid and its derivatives: Polylactic acid and its derivatives can be synthesized from renewable resources such as corn starch or sucrose. They exhibit properties analogous to those of traditional plastics and find extensive applications in the field of medical health [148]. Nevertheless, they also possess certain limitations. For instance, polylactic acid demonstrates strong hydrophobicity, which leads to poor cell affinity, thereby impeding its interaction with cells and tissue compatibility [149]. Moreover, acidic byproducts may be generated during the in vivo degradation process, causing the pH value at the implantation site to drop significantly, thus triggering an aseptic inflammatory response [150].

Polylactic acid (PLA): A linear polyester formed by the polycondensation or ring-opening polymerization of lactic acid monomers ($C_3H_6O_3$). Its degradation product is lactic acid, which is harmless to the human body. It supports minimally invasive implantation and biodegradation. When PLA is combined with chitosan (CHIT), both the mechanical strength and biodegradability of the material are improved [151].

Poly (lactic-co-glycolic acid) (PLGA): It is a copolymer of polylactic acid and polyglycolic acid. It is suitable for orthopedic implants. By adjusting the ratio of the two, PLGA can have a controllable biodegradation rate [152].

Polycaprolactone (PCL): PCL is a semi-crystalline polymer. Due to the hydrophobicity of bulk PCL, its degradation rate is relatively slow, making it suitable for implantable devices that require long-term functionality. The degradation rate of PCL can be enhanced by preparing it into electro spun fibers [153].

- Polysaccharides:

Polysaccharides represent the most abundant natural biopolymers. In recent years, they have drawn increasing attention as versatile substances applicable across diverse biomedical domains. They possess a broad spectrum of sources and relatively low costs [154]. As natural polymers, their structures bear resemblance to those of biological macromolecules such as the natural extracellular matrix, endowing them with certain potential in cell therapy [155]. Moreover, polysaccharides can serve as components of drug carriers and implantable scaffolds [156]. Nevertheless, precisely due to their natural origin, polysaccharides exhibit some limitations during certain usage scenarios that demand precise control. For instance, issues such as microbial contamination, a decline in viscosity during storage, and uncontrolled thickening and hydration rates may arise. These limitations are anticipated to be mitigated through modification [157,158].

Such as cellulose [159], chitosan [160], alginate [161], etc., have good biocompatibility and biodegradability. Researchers have conducted thorough studies on their biodegradability in the human body.

- Biomass Materials and Molecular Ferroelectric Materials:

Natural fibers, including bamboo fiber, hemp fiber, and kenaf fiber, offer renewable and biodegradable alternatives to synthetic reinforcing materials in composite materials. These fibers possess excellent mechanical properties and can be integrated into polymer matrices to enhance strength, stiffness, and durability. By means of fiber pretreatment techniques and composite formulations, the compatibility and adhesion between natural fibers and polymer matrices can be optimized, thereby enabling the preparation of sustainable composite materials suitable for a wide range of applications [162]. Nevertheless, natural biomass materials also exhibit certain drawbacks. For instance, they often display uneven performance, relatively inferior mechanical strength, and vulnerability to bacterial infection. To address these issues, researchers are actively exploring coating techniques, interface treatments, and additional modification methods [163]. The aim is to overcome these limitations and expand the performance and application scope of natural fibers in medical implant devices.

The Nair team proposed leaf skeleton-reinforced electronics as a brand-new and environmentally friendly platform for electronic devices and circuits and successfully developed a coated cellulose ethanol film that can be used for commercial reflow soldering circuits [164]. This film exhibits excellent flexibility, with a transparency of over 80% and a surface roughness of less than 5.5 nm. The advanced organic photodiodes (OPDs) and organic electrochemical transistors (OECTs) fabricated based on this film have performance similar to that of their counterparts fabricated on glass substrates. When the circuit board reaches the end of its service life, the soldered components can be conveniently separated and extracted from the substrate. The developed method can not only achieve the non-destructive recovery of electronic components, but also recycle the metals used for printed circuit interconnections without damaging the substrate itself. This research has opened up new possibilities for the application of biodegradable polymers.

As a kind of metal–organic hybrid material, the discovery of molecular ferroelectric materials has brought the piezoelectric performance of implantable piezoelectric materials to a new level. The adjacent molecules of this compound interact with each other to form a two-dimensional hydrogen bond network. This characteristic enables the HFPD crystal to exhibit excellent solubility in various solvents (especially body fluids). The compound also has good biosafety, biocompatibility, and biodegradability. Considering the brittleness and rigidity of the crystal, the Xiong research team prepared a flexible piezoelectric composite film through the solution evaporation method [129]. A controllable transient electromechanical device was assembled using this piezoelectric composite film, and it was confirmed to have good biosensing performance. This research provides a promising candidate material for degradable implantable electronic medical devices and also offers an essential application scenario closely related to human health for molecular piezoelectric materials.

There are also some materials suitable for implantable devices. The types and characteristics are detailed in Table 6.

Table 6. Classification and characteristic explanation of degradable implantable materials.

Categories	Materials	Typical Properties	Application Scenarios
Polyester	PLA	High mechanical strength, moderate degradation cycle	Intracranial pressure monitoring, cardiovascular device encapsulation
	PGA	High rigidity and rapid degradation	Orthopedic fixation monitoring, drug-controlled release system
	PLGA	Controlled degradation (weeks to years), adjustable flexibility	Tissue engineering scaffolds integrate sensors and multi-parameter biochemical monitoring
	PCL	Excellent flexibility and slow degradation (2–3 years)	Flexible hemodynamic sensors, self-powered ECG monitoring
	PHA	High biocompatibility and variable degradation cycles	Biodegradable electrode packaging, bio signal monitoring
	PHB	High crystallinity and long degradation cycle	Bone repair monitoring and implantable energy storage devices
	P4HB	High elasticity, moderate degradation cycle	Vascular stent sensor, soft tissue mechanical monitoring
	PLA-PCL	Balance strength and flexibility, adjustable degradation cycle	Multimodal sensor base, heart valve monitoring
	PLATMC	High flexibility and moderate degradation cycle	Nerve conduit pressure monitoring, soft tissue repair sensor
Polyanhydrides	PSA	Rapid degradation (weeks), surface erosion release	Short-term controlled drug release sensor, postoperative inflammation monitoring
	P(CPP-SA)	Linear drug release and controlled degradation cycle (1–6 months)	Targeted therapy sensors, tumor microenvironment monitoring
	P(FAD-SA)	Good thermal stability and non-toxic degradation products	Stress monitoring and drug release feedback of bone repair materials
	PTMC	Excellent flexibility and slow degradation (>2 years)	Vascular stent deformation monitoring, dynamic force sensor
	PPC	Good low temperature toughness, moderate degradation cycle (1–3 years)	Low temperature environment for implant device encapsulation and tissue engineering monitoring
	Chitosan	Antibacterial, rapid degradation (weeks to months)	Wound healing monitoring, infection warning sensors
	Hyaluronic Acid	High water retention, promote cell migration	Soft tissue repair monitoring, dynamic analysis of joint fluid
	Sodium Alginate	Ion-crosslinked gelation, rapid degradation (weeks)	Injectable sensor carrier, ph-responsive monitoring
	CMC	Good water solubility and high biocompatibility	Electrode paste substrate, degradable circuit board
	HPMC	Thermal gelability, moderate degradation cycle (months)	Drug sustained-release sensor, intestinal motility monitoring
	Methylcellulose	Strong film formation and rapid degradation (weeks)	Temporary encapsulation material, short-term physiological parameter monitoring
	PSA	Rapid degradation (weeks), surface erosion release	Short-term controlled drug release sensor, postoperative inflammation monitoring
Proteins	Silk Fibroin	High mechanical strength and controlled degradation cycle (3–6 months)	Flexible electrode base, neural signal monitoring
	Collagen	Promotes cell adhesion and rapid degradation (weeks)	Skin sensors, dynamic monitoring of tissue regeneration
	Gelatin	Temperature-sensitive gelation, rapid degradation (days to weeks)	Injectable sensor carrier, short-term drug release monitoring
Other Synthetic Materials	Polydioxanone	Good flexibility and moderate degradation cycle (6–12 months)	Suture tension monitoring, soft tissue repair sensor
	PGS	High elasticity, moderate degradation cycle (1–2 years)	Myocardial strain monitoring, dynamic tissue mechanics sensors
	PCLA	Balancing flexibility with degradation rate (1–3 years)	Multimodal sensor integration, organ transplant monitoring
	PLGA-PEG-PLGA	Thermosensitive gelation and degradation cycle are controllable	Injectable temperature response sensor and dynamic drug release monitoring
	(PLGA, variations in different proportions)	Adjustable degradation rate and mechanical properties (weeks to years)	Customized tissue engineering sensors, multi-parameter monitoring
	(PLGA, supplemental variant)	Rapid degradation (weeks to months), good flexibility	Short-term postoperative monitoring and inflammatory microenvironment feedback
Natural derived materials	Starch	Fast degradation (about 90 days), low cost	Temporary sensor encapsulation, gut microbial monitoring
	Lignocellulose	Natural porous structure, compostable degradation	Degradable circuit board base, environmentally responsive sensor
	Nitrocellulose	High mechanical strength, controlled degradation (months to years)	Microfluidic chip sensors, drug release monitoring

5. Degradable Devices

Based on the degradable materials introduced above, researchers have successfully developed a variety of degradable implantable devices [165–167].

Boutry used degradable Mg metal and poly (glycerol sebacate) (PGS) dielectric layer to prepare two core components of the LC resonant wireless sensor, namely the inductor and the capacitor, respectively [115]. Meanwhile, materials such as poly (3-hydroxybutyrate-co-3-hydroxyvalerate) (PHB/PHV) and poly-L-lactic acid (PLLA) were used for encapsulation and electrical isolation, endowing the sensor with both flexibility and complete degradability. This sensor can easily wrap around arteries with a diameter of less than 1 mm and can completely degrade 12 weeks after being implanted in rats, thus avoiding the need for a second surgery.

The Rogers team also developed an all-degradable LC resonant pressure sensor [79]. In this sensor, a laser-cut magnesium metal coil was used as the inductive device, zinc foil was used as the flexible electrode, and poly (lactic-co-glycolic acid) (PLGA) was used as the dielectric layer. By constructing a specific-shaped cavity structure, the deformation degree of the top electrode was effectively increased under a given applied pressure, thereby improving the sensitivity of the device. In addition, Si_3N_4 and wax were used as bioabsorbable biofluid barriers to reduce the impact of the in vivo liquid environment on the sensor (Figure 4a). This sensor remained stable during a four-day operation and exhibited the characteristics of low noise interference.

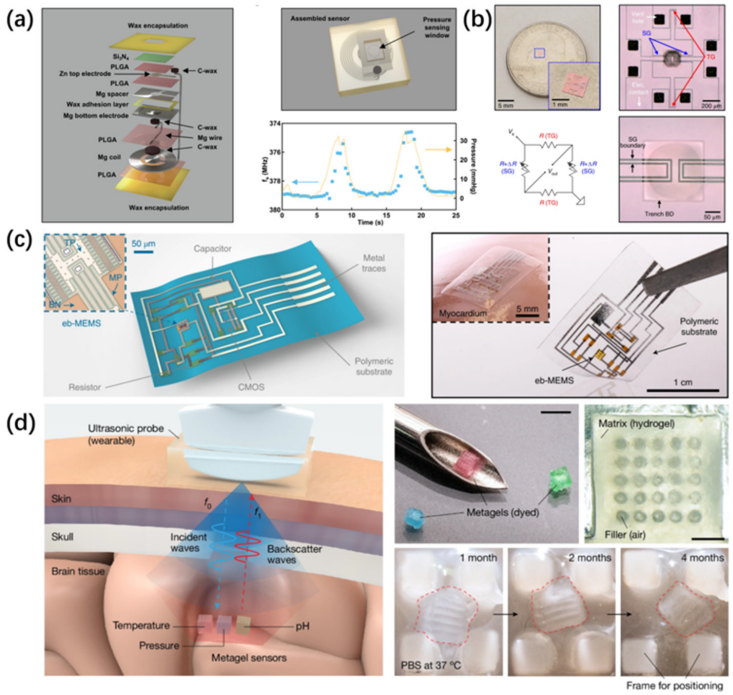


Figure 4. (**a**) The explosion view diagram of this device highlights the pressure sensing window of the sensor and the relationship between the resonant frequency and the pressure that varies over time. (**b**) Optical microscope images of the sensor and circuit diagrams of the Wheatstone bridge, consisting of strain gauges, temperature gauges, a voltage source and a meter that compensates for temperature-induced variations in the piezoresistivity of strain gauges. R represents the gauge resistance. (**c**) The highly flexible eb-MEMS platform is demonstrated, with a particular emphasis on CMOS electronic devices, resistors, capacitors, and the bioabsorbable polymer substrate. Meanwhile, the integration of this platform on the myocardial surface is presented. (**d**) Schematic diagram of the metagels wireless intracranial physiological sensor using ultrasonic reflection and its structure under the microscope. Photos of metagel degradation were displayed after one month in PBS solution at 37 °C (The dotted line depicts the shape of the meta-image).

In addition, Rogers exploited the degradable property of ultrathin silicon to develop an amorphous silica adhesive layer formed by calcining polydimethylsiloxane (PDMS), which was used to bond a pair of silicon-on-insulator (SOI) wafers to form a pressure sensor [168] (Figure 4b). This sensor used four silicon nanomembranes as the pressure/temperature sensitive regions to measure the intracranial pressure and temperature of rats. Through dissolution kinetics characterization, it was found that this sensor device could completely dissolve within 290 days without significantly affecting the performance of the sensor. The dissolved silicic acid was excreted from the body through the kidneys. Analogous to this type of system is MEMS. Leveraging specialized manufacturing processes and packaging strategies, degradable MEMS systems can be integrated onto flexible substrates. As depicted in the figure, a differential uniaxial accelerometer based on a biodegradable PAP substrate is introduced [169]. Herein, a suspended rectangular film measuring 200 μm × 420 μm × 2 μm functions as the mass block; a set of suspended serpentine structures with a cross-sectional area of 3 μm × 2 μm and a length of 2 mm act as the spring system; moreover, there are suspended interdigitated electrodes for capacitive sensing (Figure 4c). The voltage output of this device in response to periodic sinusoidal vibration aligns with both the measured values on the source silicon wafer and the theoretical values.

Beyond achieving the circuit structure using biodegradable materials, the injectable hydrogel relying on ultrasonic sensing can be rendered entirely biodegradable via a straightforward approach. Tang used a hydrogel matrix to construct periodic air columns in a 2 × 2 × 2 mm hydrogel cube, thus forming an acoustic metamaterial [170]. During practical applications, when specific-frequency ultrasonic waves are emitted by external devices, the hydrogel will undergo subtle deformations when the in vivo environment changes. This deformation causes the peak frequency of the ultrasonic reflected wave to shift. When ultrasonic waves with a peak frequency of f_0 are emitted, the super hydrogel will reflect these waves at a peak frequency of f_1 (Figure 4d). By carrying out stimulus-responsive functionalization operations (such as pressure, temperature, pH response, etc.) on the hydrogel matrix, the hydrogel can sense the changes in different physiological parameters by tracking the peak frequency shift in the reflected ultrasonic waves. This well-designed structure endows the hydrogel with excellent acoustic reflection performance, enabling it to achieve multi-parameter sensing. It is worth noting that since this device is composed only of biodegradable hydrogel and periodic air columns, this sensor can maintain normal sensing functions within 24 days after being implanted in rats and achieve complete degradation after 18 weeks.

The commercial standing of degradable medical devices exhibits a dual recovery tendency in both technology and market. Technologically, novel types of degradable medical devices are emerging in an unceasing manner. For instance, polylactic acid (PLA) is extensively applied in domains such as bone fixation devices and surgical sutures owing to its high tensile strength and favorable biocompatibility. The degradation cycle of PLA is controllable. High-molecular-weight PLA takes 2 to 5.6 years to fully degrade within the body, and its performance can be further optimized through copolymerization with other materials. Moreover, injectable PLLA products (Sculptra®, Sanofi-Aventis, Paris, France) have been approved by the FDA for the treatment of HIV-associated facial fat loss. Poly (lactic-co-glycolic acid) (PLGA) can regulate the degradation rate by adjusting the ratio of PLA to PGA and demonstrates excellent osteoconduction and osteoinduction capabilities in the orthopedic field. Polycaprolactone (PCL), due to its slow degradation rate, is suitable for long-term implants and drug delivery systems. The advantages of new degradable medical devices lie in the avoidance of secondary surgeries and the reduction in long-term risks.

For example, Lepu Medical's bioabsorbable stent (NeoVas) and Shandong Huaan's Xinsorb stent have obtained marketing approval in China [171,172]. These degradable stents are gradually assimilated by the human body after fulfilling the function of blood vessel repair. This process effectively mitigates the risks of infection and inflammation that could potentially be induced by permanent metal implants. Degradable vena cava filters possess both recovery and degradation capabilities, which significantly reduces the complication rate associated with long-term indwelling. In the orthopedic domain, degradable screws and bone plates fabricated from PLGA not only offer stable support but also facilitate bone tissue healing. As a result, the necessity for secondary surgery for removal is eliminated. The maturation and application of these technologies have broadened the market prospects of degradable medical devices and propelled the development of medical devices in a direction that is safer and more efficient.

6. Conclusions and Outlook

With the unceasing advancement of medical and electronic technologies, wireless implantable devices have evolved from theoretical concepts to practical realizations and are extensively employed in the medical domain for the monitoring of diverse physiological signals. In comparison to traditional medical devices, implantable devices possess advantages in terms of high temporal continuity and comfort during the monitoring process. The proliferation of various sensing technologies, the research breakthroughs in biodegradable materials, and the innovative designs of unique device structures have significantly propelled the robust development of this field.

This article concurrently presents the current developmental status of sensing, wireless communication, and biodegradable materials, which serve as crucial components of biodegradable implantable systems. By conducting a comparison of biodegradable materials, the article delineates the applicable scope of these materials. Specifically, a particular material is suitable for a sensor operating on a specific principle and employing a certain communication method. Through the integration of these systems, readers are enabled to design a biodegradable implantable sensor tailored to a specific scenario in accordance with their own concepts. This sensor is also characterized by high measurement accuracy and excellent communication capabilities. It is important to note that this is not merely a matter of substituting the original materials with biodegradable alternatives.

Nevertheless, numerous challenges remain to be tackled. For instance, the advancement of implantable batteries is of critical importance for prolonging the service life of devices. The design of high-performance implantable antennas has the potential to significantly enhance the range and speed of data transmission. Biodegradable silicon-based circuits also constitute a highly promising area of research. If implantable circuits can be fabricated from biodegradable materials and demonstrate performance comparable to that of traditional silicon-based solid circuits, not only will the device volume be substantially reduced, but its performance will also be notably improved. Moreover, enhancing the performance reliability of biodegradable devices is another key issue that must be surmounted. This necessitates in-depth cross-disciplinary collaboration, encompassing materials science, life science, and electronic science, to jointly drive the progress of this field. Simultaneously, it poses a significant challenge to painlessly and non-invasively implant sensors into specific locations within the human body for non-surgical patients.

In the future, implantable sensors can be widely applied to patients and sub-healthy people to continuously measure multiple physiological parameters, provide early warnings for diseases, and reduce the risk of disease deterioration.

Author Contributions: Conceptualization, Z.C. and L.P.; methodology, Z.C.; investigation, Y.Z., Q.X. and S.L.; resources, Z.C.; data curation, Z.C.; writing—original draft preparation, Z.C.; writing—review and editing, Z.C., Y.Z., Q.X. and S.L.; supervision, L.P.; project administration, L.P. All authors have read and agreed to the published version of the manuscript.

Funding: This research received no external funding.

Conflicts of Interest: The authors declare no conflict of interest.

References

1. Clausen, I.; Glott, T. Development of Clinically Relevant Implantable Pressure Sensors: Perspectives and Challenges. *Sensors* **2014**, *14*, 17686–17702. [CrossRef] [PubMed]
2. Yu, L.; Kim, B.J.; Meng, E. Chronically Implanted Pressure Sensors: Challenges and State of the Field. *Sensors* **2014**, *14*, 20620–20644. [CrossRef] [PubMed]
3. Ollmar, S.; Fernandez Schrunder, A.; Birgersson, U.; Kristoffersson, T.; Rusu, A.; Thorsson, E.; Hedenqvist, P.; Manell, E.; Rydén, A.; Jensen-Waern, M.; et al. A battery-less implantable glucose sensor based on electrical impedance spectroscopy. *Sci. Rep.* **2023**, *13*, 18122. [CrossRef] [PubMed]
4. Kim, S.; Malik, J.; Seo, J.M.; Cho, Y.M.; Bien, F. Subcutaneously implantable electromagnetic biosensor system for continuous glucose monitoring. *Sci. Rep.* **2022**, *12*, 17395. [CrossRef]
5. Wang, F.; Zhang, X.; Shokoueinejad, M.; Iskandar, B.J.; Medow, J.E.; Webster, J.G. A Novel Intracranial Pressure Readout Circuit for Passive Wireless LC Sensor. *IEEE Trans. Biomed. Circuits Syst.* **2017**, *11*, 1123–1132. [CrossRef]
6. Shin, J.; Liu, Z.; Bai, W.; Liu, Y.; Yan, Y.; Xue, Y.; Kandela, I.; Pezhouh, M.; MacEwan, M.R.; Huang, Y.; et al. Bioresorbable optical sensor systems for monitoring of intracranial pressure and temperature. *Sci. Adv.* **2019**, *5*, eaaw1899. [CrossRef]
7. Kwon, K.; Kim, J.U.; Won, S.M.; Zhao, J.; Avila, R.; Wang, H.; Chun, K.S.; Jang, H.; Lee, K.H.; Kim, J.-H.; et al. A battery-less wireless implant for the continuous monitoring of vascular pressure, flow rate and temperature. *Nat. Biomed. Eng.* **2023**, *7*, 1215–1228. [CrossRef]
8. Jang, J.; Habibagahi, I.; Mathews, R.P.; Gwak, W.; Rahmani, H.; Babakhani, A. A Wirelessly Powered, Battery-Less, and Miniaturized Microchip for Implantable Biopotential-Monitoring Applications. *IEEE Sens. J.* **2025**, *25*, 19545–19554. [CrossRef]
9. Yang, M.; Ye, Z.; Alsaab, N.; Farhat, M.; Chen, P.Y. In-Vitro Demonstration of Ultra-Reliable, Wireless and Batteryless Implanted Intracranial Sensors Operated on Loci of Exceptional Points. *IEEE Trans. Biomed. Circuits Syst.* **2022**, *16*, 287–295. [CrossRef]
10. Herbert, R.; Mishra, S.; Lim, H.-R.; Yoo, H.; Yeo, W.-H. Fully Printed, Wireless, Stretchable Implantable Biosystem toward Batteryless, Real-Time Monitoring of Cerebral Aneurysm Hemodynamics. *Adv. Sci.* **2019**, *6*, 1901034. [CrossRef]
11. Shi, B.; Liu, Z.; Zheng, Q.; Meng, J.; Ouyang, H.; Zou, Y.; Jiang, D.; Qu, X.; Yu, M.; Zhao, L.; et al. Body-Integrated Self-Powered System for Wearable and Implantable Applications. *ACS Nano* **2019**, *13*, 6017–6024. [CrossRef] [PubMed]
12. Li, Z.; Zheng, Q.; Wang, Z.L.; Li, Z. Nanogenerator-Based Self-Powered Sensors for Wearable and Implantable Electronics. *Research* **2020**, *2020*. [CrossRef] [PubMed]
13. Shukla, R.; Kiran, N.; Wang, R.; Gummeson, J.; Lee, S.I. SkinnyPower: Enabling batteryless wearable sensors via intra-body power transfer. In Proceedings of the 17th Conference on Embedded Networked Sensor Systems, New York, NY, USA, 10–13 November 2019; pp. 68–82.
14. Herrera-May, A.L.L.; Aguilera-Cortés, L.A.; García-Ramírez, P.J.; Mota-Carrillo, N.B.; Padrón-Hernández, W.Y.; Figueras, E.; Mota-Carrillo, N.B.; Padrón-Hernández, W.Y. Development of Resonant Magnetic Field Microsensors: Challenges and Future Applications. In *Microsensors*; Minin, O., Ed.; IntechOpen: Rijeka, Croatia, 2011.
15. Magkoutas, K.; Weisskopf, M.; Falk, V.; Emmert, M.Y.; Meboldt, M.; Cesarovic, N.; Schmid Daners, M. Continuous Monitoring of Blood Pressure and Vascular Hemodynamic Properties With Miniature Extravascular Hall-Based Magnetic Sensor. *JACC Basic Transl. Sci.* **2023**, *8*, 546–564. [CrossRef] [PubMed]
16. Wan, J.; Nie, Z.; Xu, J.; Zhang, Z.; Yao, S.; Xiang, Z.; Lin, X.; Lu, Y.; Xu, C.; Zhao, P.; et al. Millimeter-scale magnetic implants paired with a fully integrated wearable device for wireless biophysical and biochemical sensing. *Sci. Adv.* **2024**, *10*, eadm9314. [CrossRef]
17. Zuo, S.; Heidari, H.; Farina, D.; Nazarpour, K. Miniaturized Magnetic Sensors for Implantable Magnetomyography. *Adv. Mater. Technol.* **2020**, *5*, 2000185. [CrossRef]
18. Tan, E.L.; DeRouin, A.J.; Pereles, B.D.; Ong, K.G. Design, Fabrication, and Implementation of a Wireless, Passive Implantable Pressure Sensor Based on Magnetic Higher-Order Harmonic Fields. *Biosensors* **2011**, *1*, 134–152. [CrossRef]
19. Pan, L.; Xie, Y.; Yang, H.; Li, M.; Bao, X.; Shang, J.; Li, R.-W. Flexible Magnetic Sensors. *Sensors* **2023**, *23*, 4083. [CrossRef]
20. Zhu, K.; Kiourti, A. A Review of Magnetic Field Emissions From the Human Body: Sources, Sensors, and Uses. *IEEE Open J. Antennas Propag.* **2022**, *3*, 732–744. [CrossRef]
21. Baillet, S. Magnetoencephalography for brain electrophysiology and imaging. *Nat. Neurosci.* **2017**, *20*, 327–339. [CrossRef]

22. Kang, C.S.; Lee, Y.H.; Yu, K.K.; Kwon, H.; Kim, J.M.; Kim, K.; Lim, H.K.; Park, Y.K.; Lee, S.G. Measurement of MCG in Unshielded Environment Using a Second-Order SQUID Gradiometer. *IEEE Trans. Magn.* **2009**, *45*, 2882–2885. [CrossRef]
23. Klein, A.; van Leeuwen, P.; Hoormann, J.; Grönemeyer, D. Magnetoneurographic registration of propagating magnetic fields in the lumbar spine after stimulation of the posterior tibial nerve. *J. Neural Eng.* **2006**, *3*, 125. [CrossRef] [PubMed]
24. ter Brake, H.J.M.; Rijpma, A.P.; Stinstra, J.G.; Borgmann, J.; Holland, H.J.; Krooshoop, H.J.G.; Peters, M.J.; Flokstra, J.; Quartero, H.W.P.; Rogalla, H. Fetal magnetocardiography: Clinical relevance and feasibility. *Phys. C Supercond.* **2002**, *368*, 10–17. [CrossRef]
25. Adachi, Y.; Miyamoto, M.; Kawai, J.; Uehara, G.; Ogata, H.; Kawabata, S.; Sekihara, K.; Kado, H. Improvement of SQUID Magnetometer System for Extending Application of Spinal Cord Evoked Magnetic Field Measurement. *IEEE Trans. Appl. Supercond.* **2011**, *21*, 485–488. [CrossRef]
26. Li, J.; Quan, W.; Zhou, B.; Wang, Z.; Lu, J.; Hu, Z.; Liu, G.; Fang, J. SERF Atomic Magnetometer–Recent Advances and Applications: A Review. *IEEE Sens. J.* **2018**, *18*, 8198–8207. [CrossRef]
27. Budker, D.; Romalis, M. Optical magnetometry. *Nat. Phys.* **2007**, *3*, 227–234. [CrossRef]
28. Xia, H.; Ben-Amar Baranga, A.; Hoffman, D.; Romalis, M.V. Magnetoencephalography with an atomic magnetometer. *Appl. Phys. Lett.* **2006**, *89*, 211104. [CrossRef]
29. Li, J.-J.; Du, P.-C.; Fu, J.-Q.; Wang, X.-T.; Zhou, Q.; Wang, R.-Q. Miniature quad-channel spin-exchange relaxation-free magnetometer for magnetoencephalography*. *Chin. Phys. B* **2019**, *28*, 040703. [CrossRef]
30. Broser, P.J.; Knappe, S.; Kajal, D.S.; Noury, N.; Alem, O.; Shah, V.; Braun, C. Optically Pumped Magnetometers for Magneto-Myography to Study the Innervation of the Hand. *IEEE Trans. Neural Syst. Rehabil. Eng.* **2018**, *26*, 2226–2230. [CrossRef]
31. Morales, S.; Corsi, M.C.; Fourcault, W.; Bertrand, F.; Cauffet, G.; Gobbo, C.; Alcouffe, F.; Lenouvel, F.; Le Prado, M.; Berger, F.; et al. Magnetocardiography measurements with 4He vector optically pumped magnetometers at room temperature. *Phys. Med. Biol.* **2017**, *62*, 7267. [CrossRef]
32. Allred, J.C.; Lyman, R.N.; Kornack, T.W.; Romalis, M.V. High-Sensitivity Atomic Magnetometer Unaffected by Spin-Exchange Relaxation. *Phys. Rev. Lett.* **2002**, *89*, 130801. [CrossRef]
33. Okada, Y.C.; Shah, B.; Jin-Chu, H. Ferromagnetic high-permeability alloy alone can provide sufficient low-frequency and eddy-current shieldings for biomagnetic measurements. *IEEE Trans. Biomed. Eng.* **1994**, *41*, 688–697. [CrossRef] [PubMed]
34. Sakakibara, M.; Uehara, G.; Adachi, Y. Prediction of Cylindrical Magnetic Shielding Performance by Considering the Magnetic Field Strength Inside the Material. *IEEE Trans. Magn.* **2022**, *58*, 6500404. [CrossRef]
35. Sakakibara, M.; Uehara, G.; Adachi, Y.; Meguro, T. Evaluation of Heat Treatment of Mu-Metal Based on Permeability Under Very-Low-Frequency Micromagnetic Fields. *IEEE Trans. Magn.* **2021**, *57*, 2000204. [CrossRef]
36. Kornack, T.W.; Smullin, S.J.; Lee, S.-K.; Romalis, M.V. A low-noise ferrite magnetic shield. *Appl. Phys. Lett.* **2007**, *90*, 223501. [CrossRef]
37. Gao, Z.; Wang, X.; Zhao, Y.; Jin, Z.; Wang, G.; Gao, S. Piezoelectric-Based Smart Bone Plate for Fracture Healing Progress Monitoring. *J. Shanghai Jiaotong Univ. (Sci.)* **2022**, *27*, 561–569. [CrossRef]
38. Ali, M.; Hoseyni, S.M.; Das, R.; Awais, M.; Basdogan, I.; Beker, L. A Flexible and Biodegradable Piezoelectric-Based Wearable Sensor for Non-Invasive Monitoring of Dynamic Human Motions and Physiological Signals. *Adv. Mater. Technol.* **2023**, *8*, 2300347. [CrossRef]
39. Owida, H.A. Biomechanical Sensing Systems for Cardiac Activity Monitoring. *Int. J. Biomater.* **2022**, *2022*, 8312564. [CrossRef]
40. Curry, E.J.; Le, T.T.; Das, R.; Ke, K.; Santorella, E.M.; Paul, D.; Chorsi, M.T.; Tran, K.T.M.; Baroody, J.; Borges, E.R.; et al. Biodegradable nanofiber-based piezoelectric transducer. *Proc. Natl. Acad. Sci. USA* **2020**, *117*, 214–220. [CrossRef]
41. Yang, F.; Li, J.; Long, Y.; Zhang, Z.; Wang, L.; Sui, J.; Dong, Y.; Wang, Y.; Taylor, R.; Ni, D.; et al. Wafer-scale heterostructured piezoelectric bio-organic thin films. *Science* **2021**, *373*, 337–342. [CrossRef]
42. Chorsi, M.T.; Le, T.T.; Lin, F.; Vinikoor, T.; Das, R.; Stevens, J.F.; Mundrane, C.; Park, J.; Tran, K.T.M.; Liu, Y.; et al. Highly piezoelectric, biodegradable, and flexible amino acid nanofibers for medical applications. *Sci. Adv.* **2023**, *9*, eadg6075. [CrossRef]
43. Bhamra, H.; Huang, Y.W.; Yuan, Q.; Irazoqui, P. An Ultra-Low Power 2.4 GHz Transmitter for Energy Harvested Wireless Sensor Nodes and Biomedical Devices. *IEEE Trans. Circuits Syst. II Express Briefs* **2021**, *68*, 206–210. [CrossRef]
44. Cui, H.; Yao, D.; Hensleigh, R.; Lu, H.; Calderon, A.; Xu, Z.; Davaria, S.; Wang, Z.; Mercier, P.; Tarazaga, P.; et al. Design and printing of proprioceptive three-dimensional architected robotic metamaterials. *Science* **2022**, *376*, 1287–1293. [CrossRef] [PubMed]
45. Ma, L.L.; Chen, W.J.; Zheng, Y. Flexoelectric Effect at the Nanoscale. In *Handbook of Mechanics of Materials*; Schmauder, S., Chen, C.-S., Chawla, K.K., Chawla, N., Chen, W., Kagawa, Y., Eds.; Springer: Singapore, 2018; pp. 549–589.
46. Glinchuk, M.D.; Eliseev, E.A.; Morozovska, A.N. Spontaneous flexoelectric effect in nanosystems (topical review). *Ferroelectrics* **2016**, *500*, 90–98. [CrossRef]
47. Wang, B.; Gu, Y.; Zhang, S.; Chen, L.-Q. Flexoelectricity in solids: Progress, challenges, and perspectives. *Prog. Mater. Sci.* **2019**, *106*, 100570. [CrossRef]

48. Yan, X.; Huang, W.; Ryung Kwon, S.; Yang, S.; Jiang, X.; Yuan, F.-G. A sensor for the direct measurement of curvature based on flexoelectricity. *Smart Mater. Struct.* **2013**, *22*, 085016. [CrossRef]
49. Zhang, S.; Xu, M.; Liu, K.; Shen, S. A flexoelectricity effect-based sensor for direct torque measurement. *J. Phys. D Appl. Phys.* **2015**, *48*, 485502. [CrossRef]
50. Jia, L.; Li, L.; Guo, Z.H.; Sun, H.; Huang, H.; Sun, F.; Wang, Z.L.; Pu, X. Giant Iontronic Flexoelectricity in Soft Hydrogels Induced by Tunable Biomimetic Ion Polarization. *Adv. Mater.* **2024**, *36*, 2403830. [CrossRef]
51. Mathew, A.; Kulkarni, Y. An Electro-Chemo-Mechanical Theory With Flexoelectricity: Application to Ionic Conductivity of Soft Solid Electrolytes. *J. Appl. Mech.* **2023**, *91*, 041001. [CrossRef]
52. Sadeghi-Goughari, M.; Jeon, S.; Kwon, H.-J. Flutter instability of cantilevered carbon nanotubes caused by magnetic fluid flow subjected to a longitudinal magnetic field. *Phys. E Low-Dimens. Syst. Nanostruct.* **2018**, *98*, 184–190. [CrossRef]
53. Feng, Y.; Zhao, Y.; Yan, H.; Cai, H. A Driving Power Supply for Piezoelectric Transducers Based on an Improved LC Matching Network. *Sensors* **2023**, *23*, 5745. [CrossRef]
54. Liang, H.; Hao, G.; Olszewski, O.Z. A review on vibration-based piezoelectric energy harvesting from the aspect of compliant mechanisms. *Sens. Actuators A Phys.* **2021**, *331*, 112743. [CrossRef]
55. Deng, J.; Rorschach, K.; Baker, E.; Sun, C.; Chen, W. Topology optimization and fabrication of low frequency vibration energy harvesting microdevices. *Smart Mater. Struct.* **2015**, *24*, 025005. [CrossRef]
56. Farooq, M.; Amin, B.; Kraśny, M.J.; Elahi, A.; Rehman, M.R.U.; Wijns, W.; Shahzad, A. An Ex Vivo Study of Wireless Linkage Distance between Implantable LC Resonance Sensor and External Readout Coil. *Sensors* **2022**, *22*, 8402. [CrossRef] [PubMed]
57. Rodrigues, R.J. A experimental method to the study of wireless passive LC sensors. *Int. J. Biosens. Bioelectron.* **2018**, *4*, 175–177. [CrossRef]
58. Malik, N.A.; Sant, P.; Ajmal, T.; Ur-Rehman, M. Implantable Antennas for Bio-Medical Applications. *IEEE J. Electromagn. RF Microw. Med. Biol.* **2021**, *5*, 84–96. [CrossRef]
59. Chen, D.-Y.; Dong, L.; Huang, Q.-A. Inductor-capacitor passive wireless sensors using nonlinear parity-time symmetric configurations. *Nat. Commun.* **2024**, *15*, 9312. [CrossRef]
60. Wu, S.-Y.; Hsu, W. Design and characterization of LC strain sensors with novel inductor for sensitivity enhancement. *Smart Mater. Struct.* **2013**, *22*, 105015. [CrossRef]
61. Herbert, R.; Lim, H.-R.; Rigo, B.; Yeo, W.-H. Fully implantable wireless batteryless vascular electronics with printed soft sensors for multiplex sensing of hemodynamics. *Sci. Adv.* **2022**, *8*, eabm1175. [CrossRef]
62. Silva, N.P.; Elahi, A.; Dunne, E.; O'Halloran, M.; Amin, B. Design and Characterisation of a Read-Out System for Wireless Monitoring of a Novel Implantable Sensor for Abdominal Aortic Aneurysm Monitoring. *Sensors* **2024**, *24*, 3195. [CrossRef]
63. Zhu, J.; Jia, Y.; Li, M.; Zhou, Z.; Chen, Y.; Liu, Q.; Yang, X. A paper-based self-inductive folding displacement sensor for human respiration and motion signals measurement. *Npj Flex. Electron.* **2022**, *6*, 67. [CrossRef]
64. Dong, L.; Wang, L.F.; Huang, Q.A. A Passive Wireless Adaptive Repeater for Enhancing the Readout of LC Passive Wireless Sensors. *IEEE Microw. Wirel. Compon. Lett.* **2016**, *26*, 543–545. [CrossRef]
65. Xie, M.Z.; Wang, L.F.; Zhou, B.B.; Huang, Q.A. An Impedance Matching Method for LC Passive Wireless Sensors. *IEEE Sens. J.* **2020**, *20*, 13833–13841. [CrossRef]
66. Zhou, B.-B.; Deng, W.-J.; Wang, L.-F.; Dong, L.; Huang, Q.-A. Enhancing the Remote Distance of LC Passive Wireless Sensors by Parity-Time Symmetry Breaking. *Phys. Rev. Appl.* **2020**, *13*, 064022. [CrossRef]
67. Sakhdari, M.; Hajizadegan, M.; Li, Y.; Cheng, M.M.C.; Hung, J.C.H.; Chen, P.Y. Ultrasensitive, Parity–Time-Symmetric Wireless Reactive and Resistive Sensors. *IEEE Sens. J.* **2018**, *18*, 9548–9555. [CrossRef]
68. Ren, Q.Y.; Wang, L.F.; Huang, J.Q.; Zhang, C.; Huang, Q.A. Simultaneous Remote Sensing of Temperature and Humidity by LC-Type Passive Wireless Sensors. *J. Microelectromechanical Syst.* **2015**, *24*, 1117–1123. [CrossRef]
69. Chen, D.-Y.; Dong, L.; Huang, Q.-A. PT-Symmetric LC Passive Wireless Sensing. *Sensors* **2023**, *23*, 5191. [CrossRef]
70. Lin, M.; Hu, H.; Zhou, S.; Xu, S. Soft wearable devices for deep-tissue sensing. *Nat. Rev. Mater.* **2022**, *7*, 850–869. [CrossRef]
71. Ebrahimi, A.; Scott, J.; Ghorbani, K. Transmission Lines Terminated with LC Resonators for Differential Permittivity Sensing. *IEEE Microw. Wirel. Compon. Lett.* **2018**, *28*, 1149–1151. [CrossRef]
72. Varshney, P.K.; Kapoor, A.; Akhtar, M.J. Highly Sensitive ELC Resonator Based Differential Sensor. *IEEE Trans. Instrum. Meas.* **2021**, *70*, 8004710. [CrossRef]
73. Naqui, J.; Damm, C.; Wiens, A.; Jakoby, R.; Su, L.; Mata-Contreras, J.; Martín, F. Transmission Lines Loaded With Pairs of Stepped Impedance Resonators: Modeling and Application to Differential Permittivity Measurements. *IEEE Trans. Microw. Theory Tech.* **2016**, *64*, 3864–3877. [CrossRef]
74. Turgul, V.; Kale, I. Sensitivity of non-invasive RF/microwave glucose sensors and fundamental factors and challenges affecting measurement accuracy. In Proceedings of the 2018 IEEE International Instrumentation and Measurement Technology Conference (I2MTC), Houston, TX, USA, 14–17 May 2018; pp. 1–5.

75. Hosseini, N.; Baghelani, M. Selective real-time non-contact multi-variable water-alcohol-sugar concentration analysis during fermentation process using microwave split-ring resonator based sensor. *Sens. Actuators A Phys.* **2021**, *325*, 112695. [CrossRef]
76. Sharafadinzadeh, N.; Abdolrazzaghi, M.; Daneshmand, M. Investigation on planar microwave sensors with enhanced sensitivity from microfluidic integration. *Sens. Actuators A Phys.* **2020**, *301*, 111752. [CrossRef]
77. Carr, A.R.; Chan, Y.J.; Reuel, N.F. Contact-Free, Passive, Electromagnetic Resonant Sensors for Enclosed Biomedical Applications: A Perspective on Opportunities and Challenges. *ACS Sens.* **2023**, *8*, 943–955. [CrossRef] [PubMed]
78. Ohki, T.; Ouriel, K.; Silveira, P.G.; Katzen, B.; White, R.; Criado, F.; Diethrich, E. Initial results of wireless pressure sensing for endovascular aneurysm repair: The APEX Trial—Acute Pressure Measurement to Confirm Aneurysm Sac EXclusion. *J. Vasc. Surg.* **2007**, *45*, 236–242. [CrossRef]
79. Tian, Y.; Yang, Y.; Tang, H.; Wang, J.; Li, N.; Cheng, Y.; Kang, T.; Tang, J.; Zhou, M.; Chen, W.; et al. An implantable hydrogel-based phononic crystal for continuous and wireless monitoring of internal tissue strains. *Nat. Biomed. Eng.* **2025**, *9*, 1–14. [CrossRef]
80. Shi, C.; Andino-Pavlovsky, V.; Lee, S.A.; Costa, T.; Elloian, J.; Konofagou, E.E.; Shepard, K.L. Application of a implantable mote for in vivo real-time wireless temperature sensing. *Sci. Adv.* **2021**, *7*, eabf6312. [CrossRef]
81. Nam, J.; Byun, E.; Shim, H.; Kim, E.; Islam, S.; Park, M.; Kim, A.; Song, S.H. A Hydrogel-Based Ultrasonic Backscattering Wireless Biochemical Sensing. *Front. Bioeng. Biotechnol.* **2020**, *8*, 596370. [CrossRef]
82. Farhoudi, N.; Laurentius, L.B.; Magda, J.J.; Reiche, C.F.; Solzbacher, F. In Vivo Monitoring of Glucose Using Ultrasound-Induced Resonance in Implantable Smart Hydrogel Microstructures. *ACS Sens.* **2021**, *6*, 3587–3595. [CrossRef]
83. Huang, X.; Bell, M.A.L.; Ding, K. Deep Learning for Ultrasound Beamforming in Flexible Array Transducer. *IEEE Trans. Med. Imaging* **2021**, *40*, 3178–3189. [CrossRef]
84. Yi, J.; Nguyen, K.T.; Wang, W.; Yang, W.; Pan, M.; Lou, E.; Major, P.W.; Le, L.H.; Zeng, H. Mussel-Inspired Adhesive Double-Network Hydrogel for Intraoral Ultrasound Imaging. *ACS Appl. Bio. Mater.* **2020**, *3*, 8943–8952. [CrossRef]
85. Yi, J.; Nguyen, K.-C.T.; Wang, W.; Yang, W.; Pan, M.; Lou, E.; Major, P.W.; Le, L.H.; Zeng, H. Polyacrylamide/Alginate double-network tough hydrogels for intraoral ultrasound imaging. *J. Colloid Interface Sci.* **2020**, *578*, 598–607. [CrossRef] [PubMed]
86. La, T.-G.; Le, L.H. Flexible and Wearable Ultrasound Device for Medical Applications: A Review on Materials, Structural Designs, and Current Challenges. *Adv. Mater. Technol.* **2022**, *7*, 2100798. [CrossRef]
87. Wang, X.; Han, J.Q.; Li, G.X.; Xia, D.X.; Chang, M.Y.; Ma, X.J.; Xue, H.; Xu, P.; Li, R.J.; Zhang, K.Y.; et al. High-performance cost efficient simultaneous wireless information and power transfers deploying jointly modulated amplifying programmable metasurface. *Nat. Commun.* **2023**, *14*, 6002. [CrossRef] [PubMed]
88. Li, C.; Wu, M.; Liu, J.; Wang, R.; Wei, C.; Wang, R.; Zhou, Y.; Jiang, H.; Pan, J.; Guo, C. Noninvasive, wireless and real-time bladder pressure monitoring with biomimetic structured devices. *Appl. Mater. Today* **2022**, *29*, 101635. [CrossRef]
89. Eversense E3 Continuous Glucose Montioring System. Available online: https://www.fda.gov/medical-devices/eversense-e3-continuous-glucose-monitoring-system-p160048s016 (accessed on 17 May 2025).
90. Available online: https://nalumed.com/patients/peripheral-nerve-stimulator/ (accessed on 17 May 2025).
91. Akin, T.; Najafi, K.; Bradley, R.M. A wireless implantable multichannel digital neural recording system for a micromachined sieve electrode. *IEEE J. Solid-State Circuits* **1998**, *33*, 109–118. [CrossRef]
92. Fernandez, M.; Espinosa, H.G.; Guerra, D.; Peña, I.; Thiel, D.V.; Arrinda, A. RF Energy Absorption in Human Bodies Due to Wearable Antennas in the 2.4 GHz Frequency Band. *Bioelectromagnetics* **2020**, *41*, 73–79. [CrossRef]
93. Available online: https://www.raumedic.com/application-areas/neuromonitoring/icp-measurement/telemetry (accessed on 18 May 2025).
94. Available online: https://ichgcp.net/clinical-trials-registry/NCT00991120 (accessed on 18 May 2025).
95. Kasper, K.A.; Romero, G.F.; Perez, D.L.; Miller, A.M.; Gonzales, D.A.; Siqueiros, J.; Margolis, D.S.; Gutruf, P. Continuous operation of battery-free implants enables advanced fracture recovery monitoring. *Sci. Adv.* **2025**, *11*, eadt7488. [CrossRef]
96. Zhang, H.; Gutruf, P.; Meacham, K.; Montana, M.C.; Zhao, X.; Chiarelli, A.M.; Vázquez-Guardado, A.; Norris, A.; Lu, L.; Guo, Q.; et al. Wireless, battery-free optoelectronic systems as subdermal implants for local tissue oximetry. *Sci. Adv.* **2019**, *5*, eaaw0873. [CrossRef]
97. Available online: https://www.gentag.com/wireless-and-optical-skin-patches/ (accessed on 18 May 2025).
98. He, D.; Cui, Y.; Ming, F.; Wu, W. Advancements in Passive Wireless Sensors, Materials, Devices, and Applications. *Sensors* **2023**, *23*, 8200. [CrossRef]
99. Mohammad, I.; Huang, H. Shear sensing based on a microstrip patch antenna. *Meas. Sci. Technol.* **2012**, *23*, 105705. [CrossRef]
100. Keat Ghee, O.; Craig, A.G. A resonant printed-circuit sensor for remote query monitoring of environmental parameters. *Smart Mater. Struct.* **2000**, *9*, 421. [CrossRef]
101. Zhao, Y.; Li, Y.; Pan, B.; Kim, S.-H.; Liu, Z.; Tentzeris, M.M.; Papapolymerou, J.; Allen, M.G. RF evanescent-mode cavity resonator for passive wireless sensor applications. *Sens. Actuators A Phys.* **2010**, *161*, 322–328. [CrossRef]

102. Yue, W.; Guo, Y.; Lee, J.C.; Ganbold, E.; Wu, J.-K.; Li, Y.; Wang, C.; Kim, H.S.; Shin, Y.-K.; Liang, J.-G.; et al. Advancements in Passive Wireless Sensing Systems in Monitoring Harsh Environment and Healthcare Applications. *Nano-Micro Lett.* **2025**, *17*, 106. [CrossRef] [PubMed]
103. Wen, H.; Chen, C.; Li, S.; Shi, Y.; Wang, H.; Guo, W.; Liu, X. Array Integration and Far-Field Detection of Biocompatible Wireless LC Pressure Sensors. *Small Methods* **2021**, *5*, 2001055. [CrossRef]
104. Kalra, P.R.; Gogorishvili, I.; Khabeishvili, G.; Málek, F.; Toman, O.; Critoph, C.; Flett, A.S.; Cowburn, P.J.; Mehra, M.R.; Sheridan, W.S.; et al. First-in-Human Implantable Inferior Vena Cava Sensor for Remote Care in Heart Failure. *JACC Heart Fail.* **2025**, *13*, 1000–1010. [CrossRef]
105. Lyu, H.; Wang, J.; La, J.H.; Chung, J.M.; Babakhani, A. An Energy-Efficient Wirelessly Powered Millimeter-Scale Neurostimulator Implant Based on Systematic Codesign of an Inductive Loop Antenna and a Custom Rectifier. *IEEE Trans. Biomed. Circuits Syst.* **2018**, *12*, 1131–1143. [CrossRef]
106. Li, X.; Zhang, H.; Peng, F.; Li, Y.; Yang, T.; Wang, B.; Fang, D. A Wireless Magnetic Resonance Energy Transfer System for Micro Implantable Medical Sensors. *Sensors* **2012**, *12*, 10292–10308. [CrossRef]
107. Kim, A.; Powell, C.R.; Ziaie, B. An Implantable Pressure Sensing System With Electromechanical Interrogation Scheme. *IEEE Trans. Biomed. Eng.* **2014**, *61*, 2209–2217. [CrossRef]
108. Sheng, F.; Zhang, B.; Zhang, Y.; Li, Y.; Cheng, R.; Wei, C.; Ning, C.; Dong, K.; Wang, Z.L. Ultrastretchable Organogel/Silicone Fiber-Helical Sensors for Self-Powered Implantable Ligament Strain Monitoring. *ACS Nano* **2022**, *16*, 10958–10967. [CrossRef]
109. Mohan, A.; Kumar, N. Implantable antennas for biomedical applications: A systematic review. *Biomed. Eng. OnLine* **2024**, *23*, 87. [CrossRef]
110. Karacolak, T.; Hood, A.Z.; Topsakal, E. Design of a Dual-Band Implantable Antenna and Development of Skin Mimicking Gels for Continuous Glucose Monitoring. *IEEE Trans. Microw. Theory Tech.* **2008**, *56*, 1001–1008. [CrossRef]
111. Tawk, Y. A Dynamic Dual Tapered 3-D Printed Nested Helical Antenna. *IEEE Trans. Antennas Propag.* **2020**, *68*, 697–702. [CrossRef]
112. Lamkaddem, A.; Yousfi, A.E.; Abdalmalak, K.A.; Posadas, V.G.; Segovia-Vargas, D. Circularly Polarized Miniaturized Implantable Antenna for Leadless Pacemaker Devices. *IEEE Trans. Antennas Propag.* **2022**, *70*, 6423–6432. [CrossRef]
113. Yang, X.T.; Wong, H.; Xiang, J. Polarization Reconfigurable Planar Inverted-F Antenna for Implantable Telemetry Applications. *IEEE Access* **2019**, *7*, 141900–141909. [CrossRef]
114. Permana, H.; Fang, Q.; Cosic, I. 3-layer implantable microstrip antenna optimised for retinal prosthesis system in MICS band. In Proceedings of the International Symposium on Bioelectronics and Bioinformations 2011, Suzhou, China, 3–5 November 2011; pp. 65–68.
115. Boutry, C.M.; Beker, L.; Kaizawa, Y.; Vassos, C.; Tran, H.; Hinckley, A.C.; Pfattner, R.; Niu, S.; Li, J.; Claverie, J.; et al. Biodegradable and flexible arterial-pulse sensor for the wireless monitoring of blood flow. *Nat. Biomed. Eng.* **2019**, *3*, 47–57. [CrossRef]
116. Khan, M.W.A.; Moradi, E.; Sydänheimo, L.; Björninen, T.; Rahmat-Samii, Y.; Ukkonen, L. Miniature Coplanar Implantable Antenna on Thin and Flexible Platform for Fully Wireless Intracranial Pressure Monitoring System. *Int. J. Antennas Propag.* **2017**, *2017*, 9161083. [CrossRef]
117. Wang, M.; Yang, Z.; Wu, J.; Bao, J.; Liu, J.; Cai, L.; Dang, T.; Zheng, H.; Li, E. Investigation of SAR Reduction Using Flexible Antenna With Metamaterial Structure in Wireless Body Area Network. *IEEE Trans. Antennas Propag.* **2018**, *66*, 3076–3086. [CrossRef]
118. *ISO 10993-1:2018*; Quality Management Systems—Requirements. ISO: Geneva, Switzerland, 2018.
119. Xu, K.; Li, S.; Dong, S.; Zhang, S.; Pan, G.; Wang, G.; Shi, L.; Guo, W.; Yu, C.; Luo, J. Bioresorbable Electrode Array for Electrophysiological and Pressure Signal Recording in the Brain. *Adv. Healthc. Mater.* **2019**, *8*, 1801649. [CrossRef]
120. Zhang, C.; Wen, T.H.; Razak, K.A.; Lin, J.; Villafana, E.; Jimenez, H.; Liu, H. Fabrication and Characterization of Biodegradable Metal Based Microelectrodes for In Vivo Neural Recording. *MRS Adv.* **2019**, *4*, 2471–2477. [CrossRef]
121. Zhu, Y.; Zhang, H.; Zhang, Y.; Wu, H.; Wei, L.; Zhou, G.; Zhang, Y.; Deng, L.; Cheng, Y.; Li, M.; et al. Endovascular Metal Devices for the Treatment of Cerebrovascular Diseases. *Adv. Mater.* **2019**, *31*, 1805452. [CrossRef]
122. Toong, D.W.Y.; Ng, J.C.K.; Huang, Y.; Wong, P.E.H.; Leo, H.L.; Venkatraman, S.S.; Ang, H.Y. Bioresorbable metals in cardiovascular stents: Material insights and progress. *Materialia* **2020**, *12*, 100727. [CrossRef]
123. Wei, S.; Ma, J.-X.; Xu, L.; Gu, X.-S.; Ma, X.-L. Biodegradable materials for bone defect repair. *Mil. Med. Res.* **2020**, *7*, 54. [CrossRef] [PubMed]
124. Han, H.-S.; Jun, I.; Seok, H.-K.; Lee, K.-S.; Lee, K.; Witte, F.; Mantovani, D.; Kim, Y.-C.; Glyn-Jones, S.; Edwards, J.R. Biodegradable Magnesium Alloys Promote Angio-Osteogenesis to Enhance Bone Repair. *Adv. Sci.* **2020**, *7*, 2000800. [CrossRef] [PubMed]
125. Rüegg, M.; Blum, R.; Boero, G.; Brugger, J. Biodegradable Frequency-Selective Magnesium Radio-Frequency Microresonators for Transient Biomedical Implants. *Adv. Funct. Mater.* **2019**, *29*, 1903051. [CrossRef]
126. Lu, D.; Yan, Y.; Deng, Y.; Yang, Q.; Zhao, J.; Seo, M.-H.; Bai, W.; MacEwan, M.R.; Huang, Y.; Ray, W.Z.; et al. Bioresorbable Wireless Sensors as Temporary Implants for In Vivo Measurements of Pressure. *Adv. Funct. Mater.* **2020**, *30*, 2003754. [CrossRef]

127. Wu, C.; Lin, F.; Liu, H.; Pelletier, M.H.; Lloyd, M.; Walsh, W.R.; Nie, J.-F. Stronger and coarser-grained biodegradable zinc alloys. *Nature* **2025**, *638*, 684–689. [CrossRef]
128. Zhang, F.; Zheng, Y.; Wang, L.; Kang, Y.; Dong, H.; Li, H.; Zhao, X.; Li, B.; Chen, H.; Qiu, J.; et al. Implantable Zinc Ion Battery and Osteogenesis-Immunoregulation Bifunction of Its Catabolite. *ACS Nano* **2024**, *18*, 21246–21257. [CrossRef]
129. Zhang, H.-Y.; Tang, Y.-Y.; Gu, Z.-X.; Wang, P.; Chen, X.-G.; Lv, H.-P.; Li, P.-F.; Jiang, Q.; Gu, N.; Ren, S.; et al. Biodegradable ferroelectric molecular crystal with large piezoelectric response. *Science* **2024**, *383*, 1492–1498. [CrossRef]
130. Sheng, H.; Zhou, J.; Li, B.; He, Y.; Zhang, X.; Liang, J.; Zhou, J.; Su, Q.; Xie, E.; Lan, W.; et al. A thin, deformable, high-performance supercapacitor implant that can be biodegraded and bioabsorbed within an animal body. *Sci. Adv.* **2021**, *7*, eabe3097. [CrossRef]
131. Shao, M.; Sheng, H.; Lin, L.; Ma, H.; Wang, Q.; Yuan, J.; Zhang, X.; Chen, G.; Li, W.; Su, Q.; et al. High-Performance Biodegradable Energy Storage Devices Enabled by Heterostructured MoO_3–MoS_2 Composites. *Small* **2023**, *19*, 2205529. [CrossRef]
132. Mohamed, A.; El-Aziz, A.M.; Breitinger, H.-G. Study of the degradation behavior and the biocompatibility of Mg–0.8Ca alloy for orthopedic implant applications. *J. Magnes. Alloys* **2019**, *7*, 249–257. [CrossRef]
133. Redlich, C.; Schauer, A.; Scheibler, J.; Poehle, G.; Barthel, P.; Maennel, A.; Adams, V.; Weissgaerber, T.; Linke, A.; Quadbeck, P. In Vitro Degradation Behavior and Biocompatibility of Bioresorbable Molybdenum. *Metals* **2021**, *11*, 761. [CrossRef]
134. Zhu, S.; Huang, N.; Xu, L.; Zhang, Y.; Liu, H.; Sun, H.; Leng, Y. Biocompatibility of pure iron: In vitro assessment of degradation kinetics and cytotoxicity on endothelial cells. *Mater. Sci. Eng. C* **2009**, *29*, 1589–1592. [CrossRef]
135. Törne, K.; Larsson, M.; Norlin, A.; Weissenrieder, J. Degradation of zinc in saline solutions, plasma, and whole blood. *J. Biomed. Mater. Res. Part B Appl. Biomater.* **2016**, *104*, 1141–1151. [CrossRef]
136. Yin, L.; Bozler, C.; Harburg, D.V.; Omenetto, F.; Rogers, J.A. Materials and fabrication sequences for water soluble silicon integrated circuits at the 90 nm node. *Appl. Phys. Lett.* **2015**, *106*, 014105. [CrossRef]
137. Lee, Y.K.; Yu, K.J.; Song, E.; Barati Farimani, A.; Vitale, F.; Xie, Z.; Yoon, Y.; Kim, Y.; Richardson, A.; Luan, H.; et al. Dissolution of Monocrystalline Silicon Nanomembranes and Their Use as Encapsulation Layers and Electrical Interfaces in Water-Soluble Electronics. *ACS Nano* **2017**, *11*, 12562–12572. [CrossRef]
138. Shao, Y.; Hu, B.; Liu, X.; Ni, Z.; Shu, Y.; Zhang, X.; Shen, J.; Liang, L.; Zhou, L.; Liu, J.; et al. Multi-functional, conformal systems with ultrathin crystalline-silicon-based bioelectronics for characterization of intraocular pressure and ocular surface temperature. *Biosens. Bioelectron.* **2025**, *267*, 116786. [CrossRef]
139. Wu, M.; Yao, K.; Huang, N.; Li, H.; Zhou, J.; Shi, R.; Li, J.; Huang, X.; Li, J.; Jia, H.; et al. Ultrathin, Soft, Bioresorbable Organic Electrochemical Transistors for Transient Spatiotemporal Mapping of Brain Activity. *Adv. Sci.* **2023**, *10*, 2300504. [CrossRef]
140. Mempin, M.; Hu, H.; Chowdhury, D.; Deva, A.; Vickery, K. The A, B and C's of Silicone Breast Implants: Anaplastic Large Cell Lymphoma, Biofilm and Capsular Contracture. *Materials* **2018**, *11*, 2393. [CrossRef]
141. Zappi, E.; Barnett, J.G.; Zappi, M.; Barnett, C.R. The Long-Term Host Response to Liquid Silicone Injected during Soft Tissue Augmentation Procedures: A Microscopic Appraisal. *Dermatol. Surg.* **2007**, *33*, S186–S192. [CrossRef]
142. Lee, J.C.; Heo, C.Y. Implementing Tissue Engineering and Regenerative Medicine Solutions in Silicone Implants. In *Regenerative Medicine and Plastic Surgery: Elements, Research Concepts and Emerging Technologies*; Duscher, D., Shiffman, M.A., Eds.; Springer International Publishing: Cham, Switzerland, 2019; pp. 303–318.
143. Li, M.; Neoh, K.G.; Xu, L.Q.; Wang, R.; Kang, E.-T.; Lau, T.; Olszyna, D.P.; Chiong, E. Surface Modification of Silicone for Biomedical Applications Requiring Long-Term Antibacterial, Antifouling, and Hemocompatible Properties. *Langmuir* **2012**, *28*, 16408–16422. [CrossRef] [PubMed]
144. Yesilirmak, N.; Altınors, D.D. A silicone hydrogel contact lens after 7 years of continuous wear. *Contact Lens Anterior Eye* **2013**, *36*, 204–206. [CrossRef] [PubMed]
145. Hwang, S.-W.; Tao, H.; Kim, D.-H.; Cheng, H.; Song, J.-K.; Rill, E.; Brenckle, M.A.; Panilaitis, B.; Won, S.M.; Kim, Y.-S.; et al. A Physically Transient Form of Silicon Electronics. *Science* **2012**, *337*, 1640–1644. [CrossRef]
146. Tao, H.; Hwang, S.-W.; Marelli, B.; An, B.; Moreau, J.E.; Yang, M.; Brenckle, M.A.; Kim, S.; Kaplan, D.L.; Rogers, J.A.; et al. Silk-based resorbable electronic devices for remotely controlled therapy and in vivo infection abatement. *Proc. Natl. Acad. Sci. USA* **2014**, *111*, 17385–17389. [CrossRef]
147. Li, C.; Guo, C.; Fitzpatrick, V.; Ibrahim, A.; Zwierstra, M.J.; Hanna, P.; Lechtig, A.; Nazarian, A.; Lin, S.J.; Kaplan, D.L. Design of biodegradable, implantable devices towards clinical translation. *Nat. Rev. Mater.* **2020**, *5*, 61–81. [CrossRef]
148. Ranakoti, L.; Gangil, B.; Mishra, S.K.; Singh, T.; Sharma, S.; Ilyas, R.A.; El-Khatib, S. Critical Review on Polylactic Acid: Properties, Structure, Processing, Biocomposites, and Nanocomposites. *Materials* **2022**, *15*, 4312. [CrossRef]
149. Esmaeili, M.; Pircheraghi, G.; Bagheri, R.; Altstädt, V. Poly(lactic acid)/coplasticized thermoplastic starch blend: Effect of plasticizer migration on rheological and mechanical properties. *Polym. Adv. Technol.* **2019**, *30*, 839–851. [CrossRef]
150. Sickles, C.K.; Nassereddin, A.; Patel, P.; Gross, G.P. *Poly-L-Lactic Acid*; StatPearls: Tampa/St. Petersburg, FL, USA, 2024.
151. Valencia, C.H. Hydrolytic degradation and in vivo resorption of poly-<l-lactic acid-chitosan biomedical devices in the parietal bones of Wistar rats. *J. Int. Med. Res.* **2019**, *47*, 1705–1716. [CrossRef]

152. Yoon, S.-K.; Chung, D.-J. In Vivo Degradation Studies of PGA-PLA Block Copolymer and Their Histochemical Analysis for Spinal-Fixing Application. *Polymers* **2022**, *14*, 3322. [CrossRef]
153. Dias, J.R.; Sousa, A.; Augusto, A.; Bártolo, P.J.; Granja, P.L. Electrospun Polycaprolactone (PCL) Degradation: An In Vitro and In Vivo Study. *Polymers* **2022**, *14*, 3397. [CrossRef]
154. Shariatinia, Z. Chapter 2-Pharmaceutical applications of natural polysaccharides. In *Natural Polysaccharides in Drug Delivery and Biomedical Applications*; Hasnain, M.S., Nayak, A.K., Eds.; Academic Press: Cambridge, MA, USA, 2019; pp. 15–57.
155. Darge, H.F.; Andrgie, A.T.; Tsai, H.-C.; Lai, J.-Y. Polysaccharide and polypeptide based injectable thermo-sensitive hydrogels for local biomedical applications. *Int. J. Biol. Macromol.* **2019**, *133*, 545–563. [CrossRef] [PubMed]
156. Ren, Y.; Bai, Y.; Zhang, Z.; Cai, W.; Del Rio Flores, A. The Preparation and Structure Analysis Methods of Natural Polysaccharides of Plants and Fungi: A Review of Recent Development. *Molecules* **2019**, *24*, 3122. [CrossRef] [PubMed]
157. Saidin, N.M.; Anuar, N.K.; Affandi, M.M. Roles of Polysaccharides in Transdermal Drug Delivery System and Future Prospects. *J. Appl. Pharm. Sci.* **2018**, *8*, 141–157. [CrossRef]
158. van Dam, J.E.G.; van den Broek, L.A.M.; Boeriu, C.G. Polysaccharides in Human Health Care. *Nat. Prod. Commun.* **2017**, *12*, 1934578X1701200604. [CrossRef]
159. Moraïs, S.; Winkler, S.; Zorea, A.; Levin, L.; Nagies, F.S.P.; Kapust, N.; Lamed, E.; Artan-Furman, A.; Bolam, D.N.; Yadav, M.P.; et al. Cryptic diversity of cellulose-degrading gut bacteria in industrialized humans. *Science* **2024**, *383*, eadj9223. [CrossRef]
160. Niu, Y.; Hu, W. Preparation, characterization and application in environmental protection of low-molecular-weight chitosan: A review. *Sustain. Environ. Res.* **2024**, *34*, 29. [CrossRef]
161. Rivas-Fernández, J.P.; Vuillemin, M.; Pilgaard, B.; Klau, L.J.; Fredslund, F.; Lund-Hanssen, C.; Welner, D.H.; Meyer, A.S.; Morth, J.P.; Meilleur, F.; et al. Unraveling the molecular mechanism of polysaccharide lyases for efficient alginate degradation. *Nat. Commun.* **2025**, *16*, 2670. [CrossRef]
162. Elfaleh, I.; Abbassi, F.; Habibi, M.; Ahmad, F.; Guedri, M.; Nasri, M.; Garnier, C. A comprehensive review of natural fibers and their composites: An eco-friendly alternative to conventional materials. *Results Eng.* **2023**, *19*, 101271. [CrossRef]
163. Zwawi, M. A Review on Natural Fiber Bio-Composites, Surface Modifications and Applications. *Molecules* **2021**, *26*, 404. [CrossRef]
164. Nair, R.R.; Wolansky, J.; Uhlig, K.; Solgi, A.; Teuerle, L.; Zhang, T.; Schröder, J.; Antrack, T.; Benduhn, J.; Kleemann, H.; et al. Leaftronics: Natural lignocellulose scaffolds for sustainable electronics. *Sci. Adv.* **2024**, *10*, eadq3276. [CrossRef]
165. Sheng, H.; Jiang, L.; Wang, Q.; Zhang, Z.; Lv, Y.; Ma, H.; Bi, H.; Yuan, J.; Shao, M.; Li, F.; et al. A soft implantable energy supply system that integrates wireless charging and biodegradable Zn-ion hybrid supercapacitors. *Sci. Adv.* **2023**, *9*, eadh8083. [CrossRef] [PubMed]
166. Li, H.; Zhao, C.; Wang, X.; Meng, J.; Zou, Y.; Noreen, S.; Zhao, L.; Liu, Z.; Ouyang, H.; Tan, P.; et al. Fully Bioabsorbable Capacitor as an Energy Storage Unit for Implantable Medical Electronics. *Adv. Sci.* **2019**, *6*, 1801625. [CrossRef] [PubMed]
167. Zheng, Q.; Zou, Y.; Zhang, Y.; Liu, Z.; Shi, B.; Wang, X.; Jin, Y.; Ouyang, H.; Li, Z.; Wang, Z.L. Biodegradable triboelectric nanogenerator as a life-time designed implantable power source. *Sci. Adv.* **2016**, *2*, e1501478. [CrossRef] [PubMed]
168. Shin, J.; Yan, Y.; Bai, W.; Xue, Y.; Gamble, P.; Tian, L.; Kandela, I.; Haney, C.R.; Spees, W.; Lee, Y.; et al. Bioresorbable pressure sensors protected with thermally grown silicon dioxide for the monitoring of chronic diseases and healing processes. *Nat. Biomed. Eng.* **2019**, *3*, 37–46. [CrossRef]
169. Yang, Q.; Liu, T.-L.; Xue, Y.; Wang, H.; Xu, Y.; Emon, B.; Wu, M.; Rountree, C.; Wei, T.; Kandela, I.; et al. Ecoresorbable and bioresorbable microelectromechanical systems. *Nat. Electron.* **2022**, *5*, 526–538. [CrossRef]
170. Tang, H.; Yang, Y.; Liu, Z.; Li, W.; Zhang, Y.; Huang, Y.; Kang, T.; Yu, Y.; Li, N.; Tian, Y.; et al. Injectable ultrasonic sensor for wireless monitoring of intracranial signals. *Nature* **2024**, *630*, 84–90. [CrossRef]
171. Han, Y.; Xu, B.; Fu, G.; Wang, X.; Xu, K.; Jin, C.; Tao, L.; Li, L.; Hou, Y.; Su, X.; et al. A Randomized Trial Comparing the NeoVas Sirolimus-Eluting Bioresorbable Scaffold and Metallic Everolimus-Eluting Stents. *JACC Cardiovasc. Interv.* **2018**, *11*, 260–272. [CrossRef]
172. Wu, Y.; Yin, J.; Chen, J.; Yao, Z.; Qian, J.; Shen, L.; Ge, L.; Ge, J. Final report of the 5-year clinical outcomes of the XINSORB bioresorbable sirolimus-eluting scaffold in the treatment of single de novo coronary lesions in a first-in-human study. *Ann. Transl. Med.* **2020**, *8*, 1162. [CrossRef]

Disclaimer/Publisher's Note: The statements, opinions and data contained in all publications are solely those of the individual author(s) and contributor(s) and not of MDPI and/or the editor(s). MDPI and/or the editor(s) disclaim responsibility for any injury to people or property resulting from any ideas, methods, instructions or products referred to in the content.